Topics on Galaxy Clusters

Gastão B. Lima Neto – IAG/USP

VII Escola José Plínio Baptista de Cosmologia
Pedra Azul/ES, 23-27/11/2024

Topics

- What are galaxy clusters?
- Properties (galaxies, ICM)
- X-ray observations
- Hydrostatic mass and cooling-flow
- Scaling relations
- Cluster collisions
- High-z clusters and proto-clusters
- Future X-ray mission

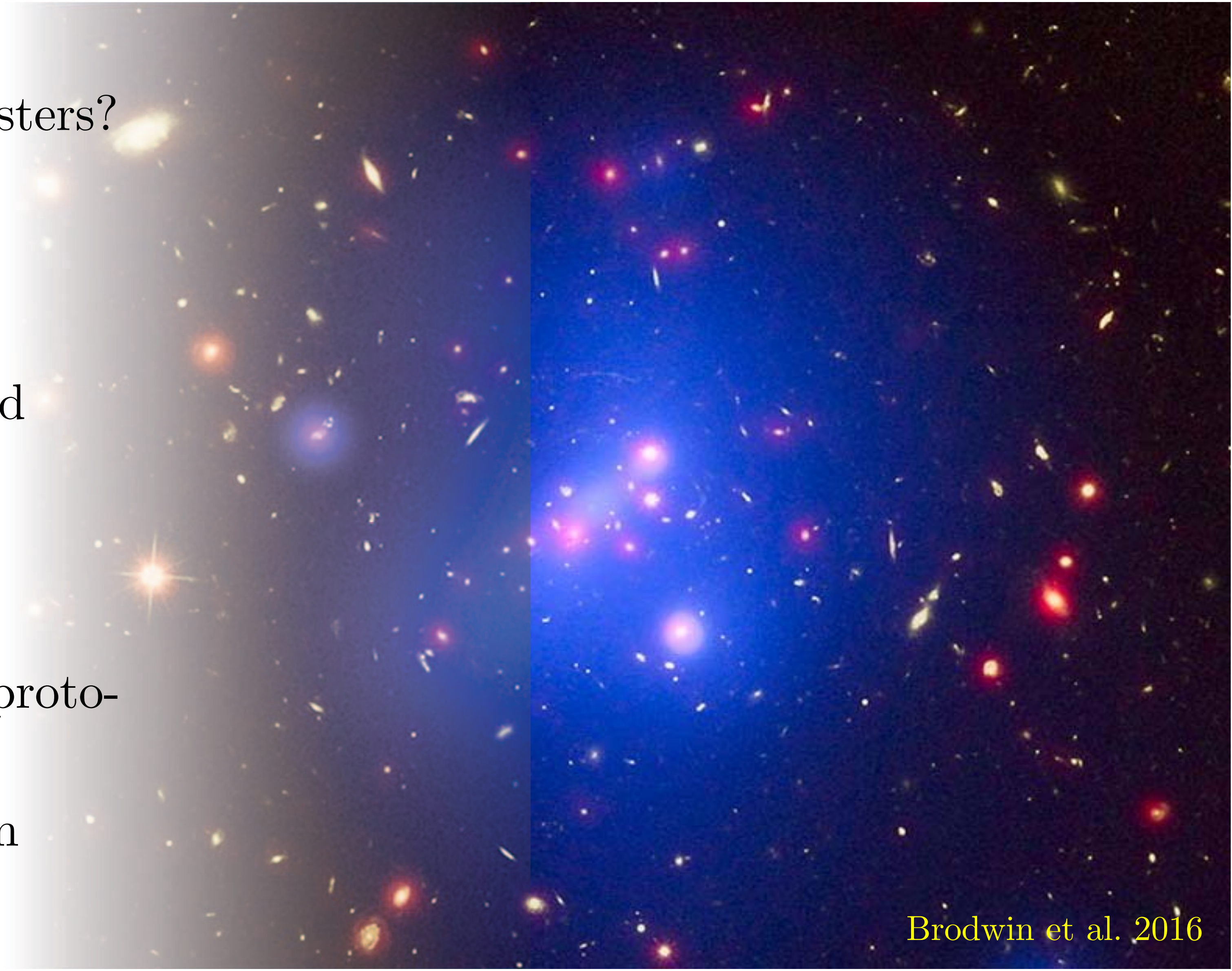

IDCS J1426.5+3508; *Chandra*+HST+*Spitzer*; $z = 1.75$

Clusters of galaxies ➔ Dark matter halos

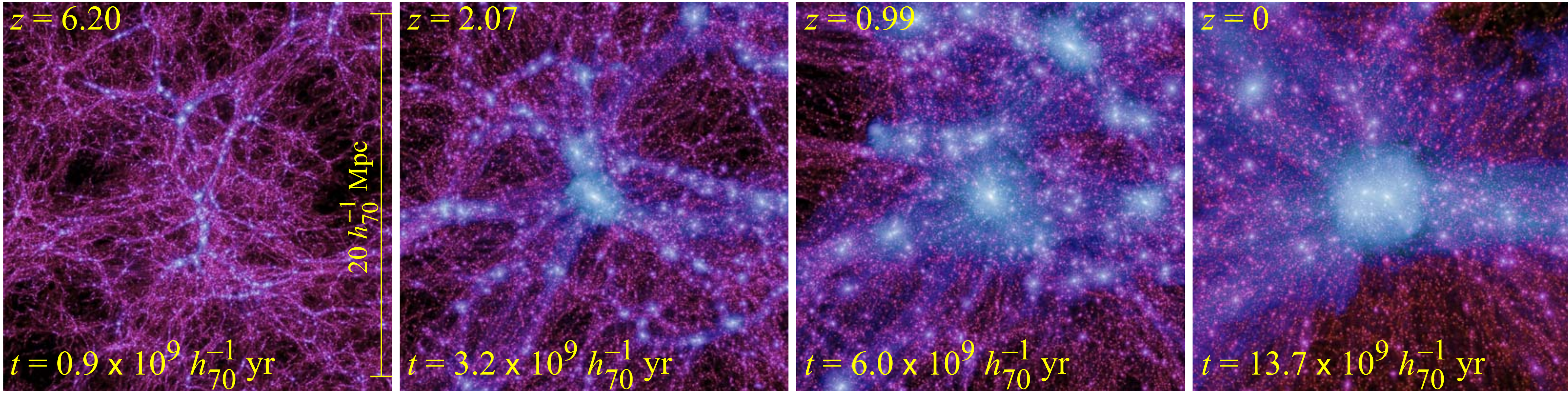

- Clusters => Intersection/nodes on the CDM cosmic filaments

- Hierarchical scenario of large-scale structure formation (ΛCDM Universe):
  => Clusters are still forming;
  => Infall of matter along the cosmic filaments.

Large scale structure formation

ΛCDM scenario ➔ Hierarchical formation, from small to large scale

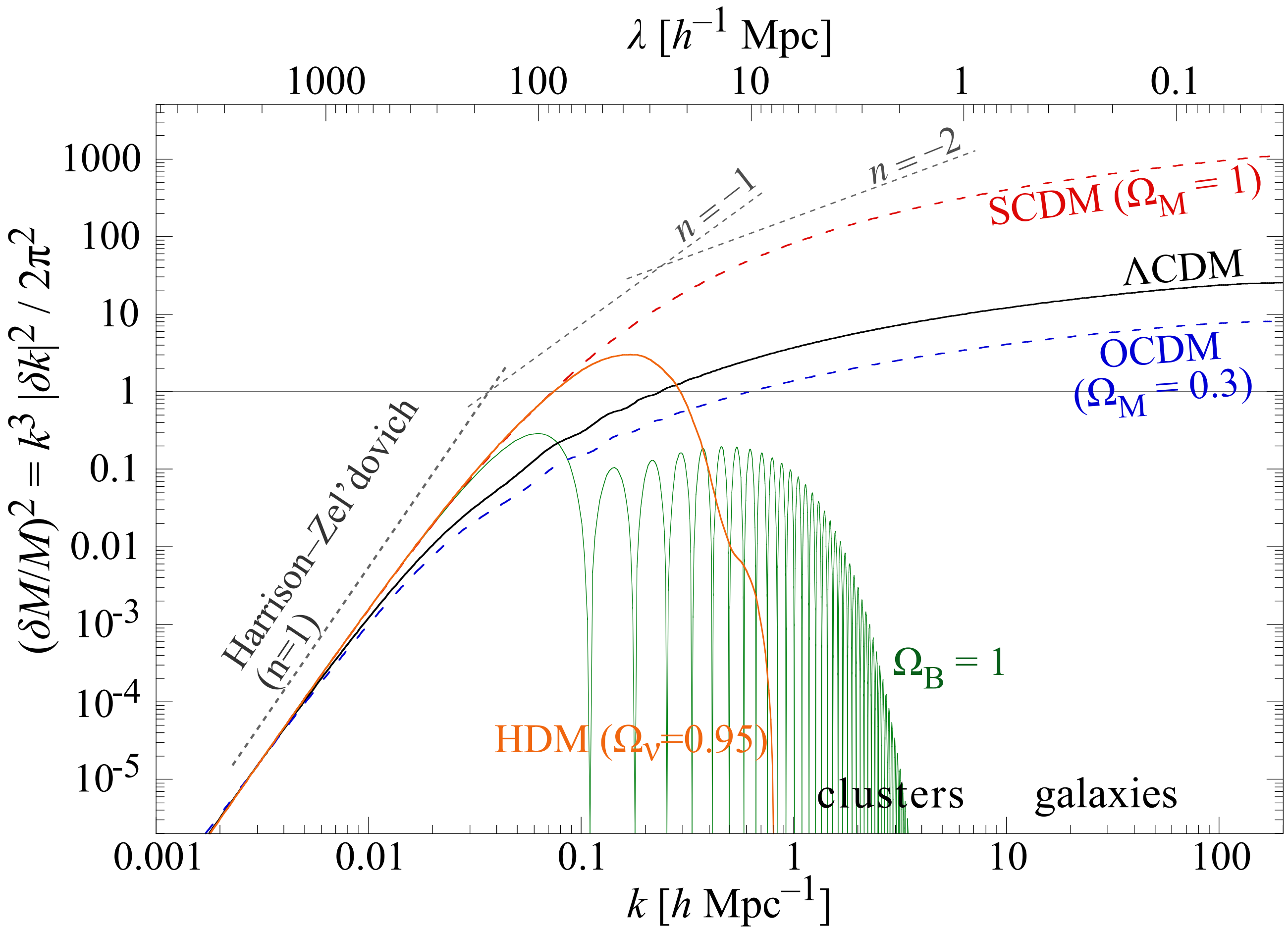

Power spectrum of density fluctuations

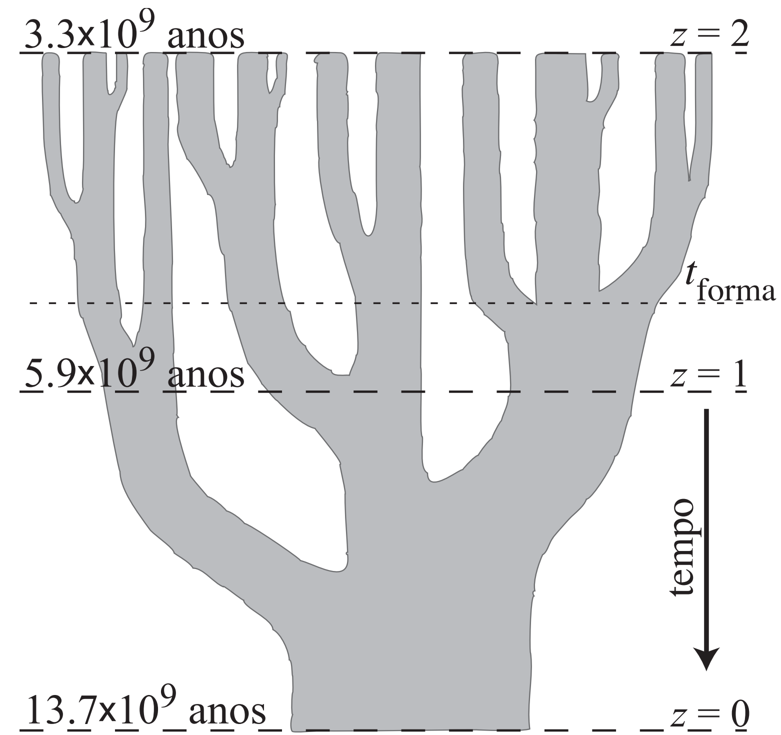

"**merging tree**" showing the events leading to the formation of a massive halo at $z = 0$ (Lacey & Cole 1993).

Definitions

- Rich clusters: $\approx 10^3$ galaxies, $M \approx 10^{15}\ M_\odot$.
- Poor clusters: $\approx 10^2$ galaxies, $M \approx 10^{14}\ M_\odot$.
  - ✓ definition overlaps that of rich groups.
- Size: $R \approx 1$–2 Mpc.
  - ✓ Central region (core) $\approx$ 50–150kpc.
- Mean matter density: $\approx 200 \times \rho_c$
  - ✓ ($\approx 2000 \times \rho_c$ in central region).
- Relatively rare, they contain $\approx 7\%$ of all galaxies.
- Young objects: formation (collapse) around $z \leq 2$.
- Dynamical time scale: $R/\sigma \sim 10^9$ yr.

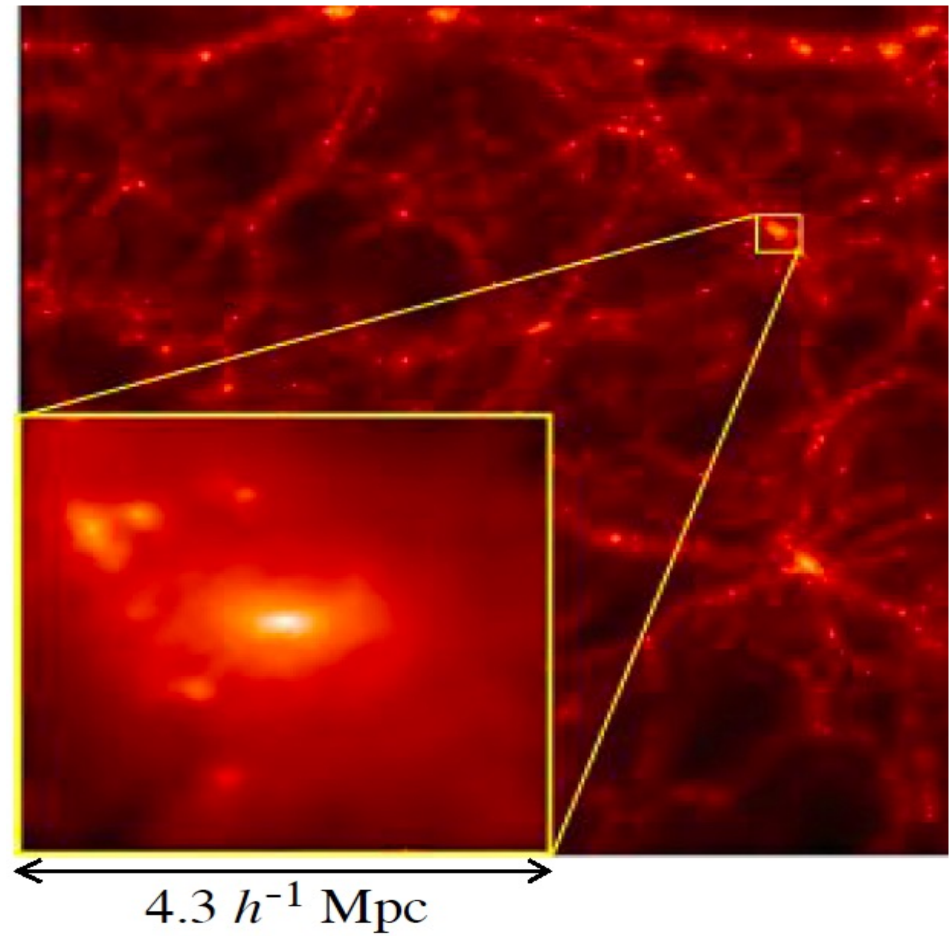

Abell 3376

z = 0.0456; “true-color” *grz* DECam/Blanco/CTIO image

Coma: most massive cluster in the local Universe

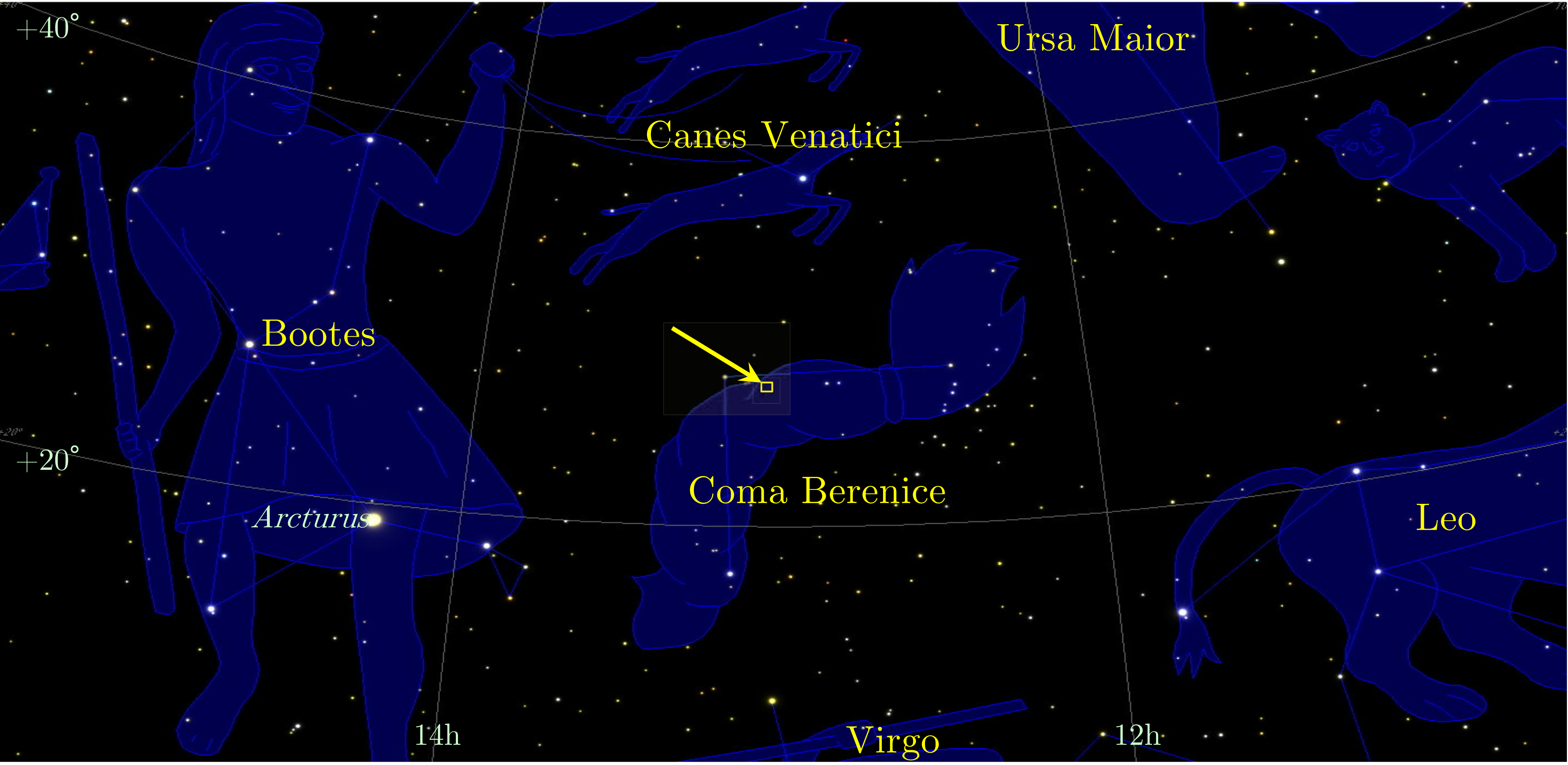

Coma: most massive cluster in the local Universe

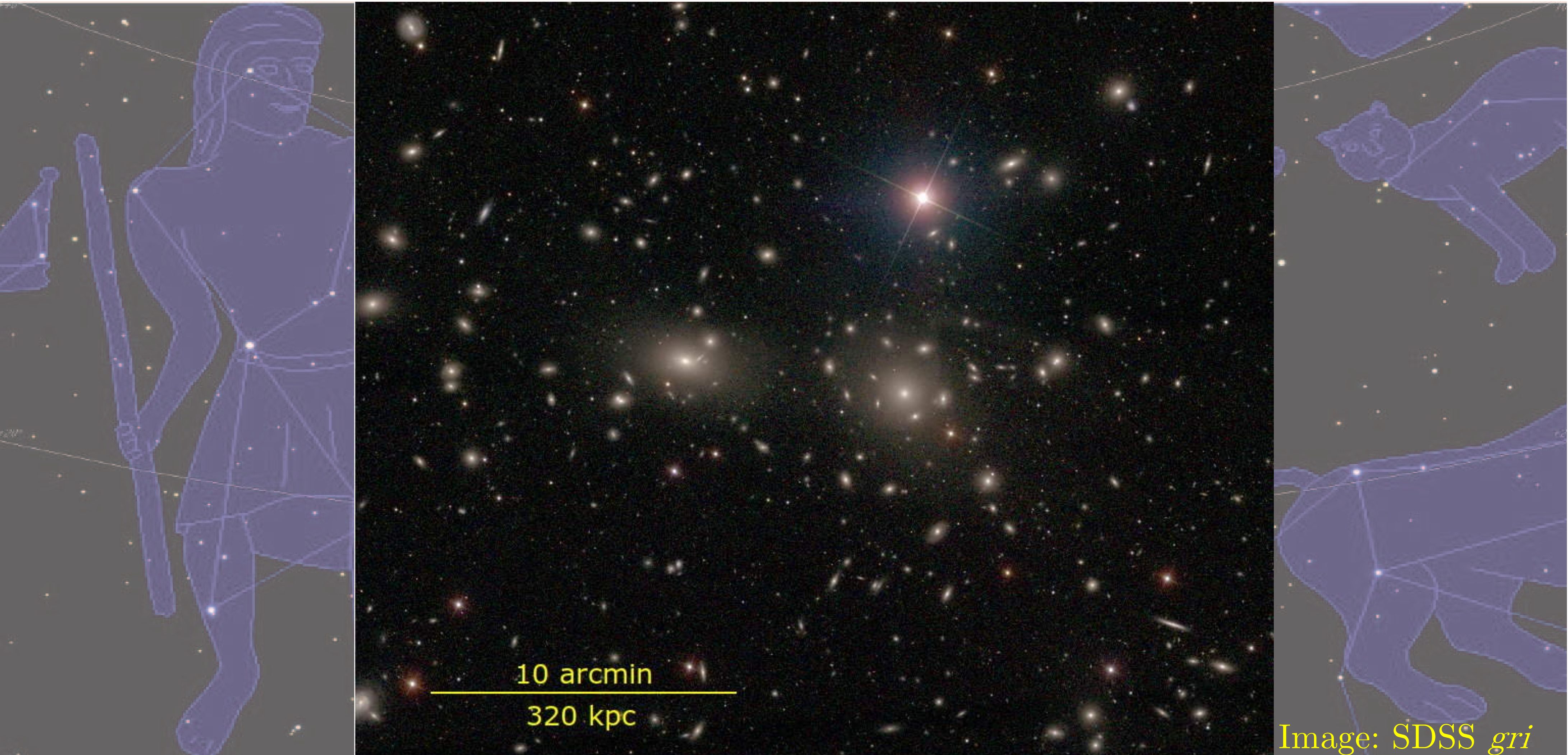

Central Region, ≈ 0.5 Mpc. Distance ≈ 110 Mpc. Total Mass ≈ 2.5–3.0 $\times 10^{15}\ M_{\odot}$.

Mass composition

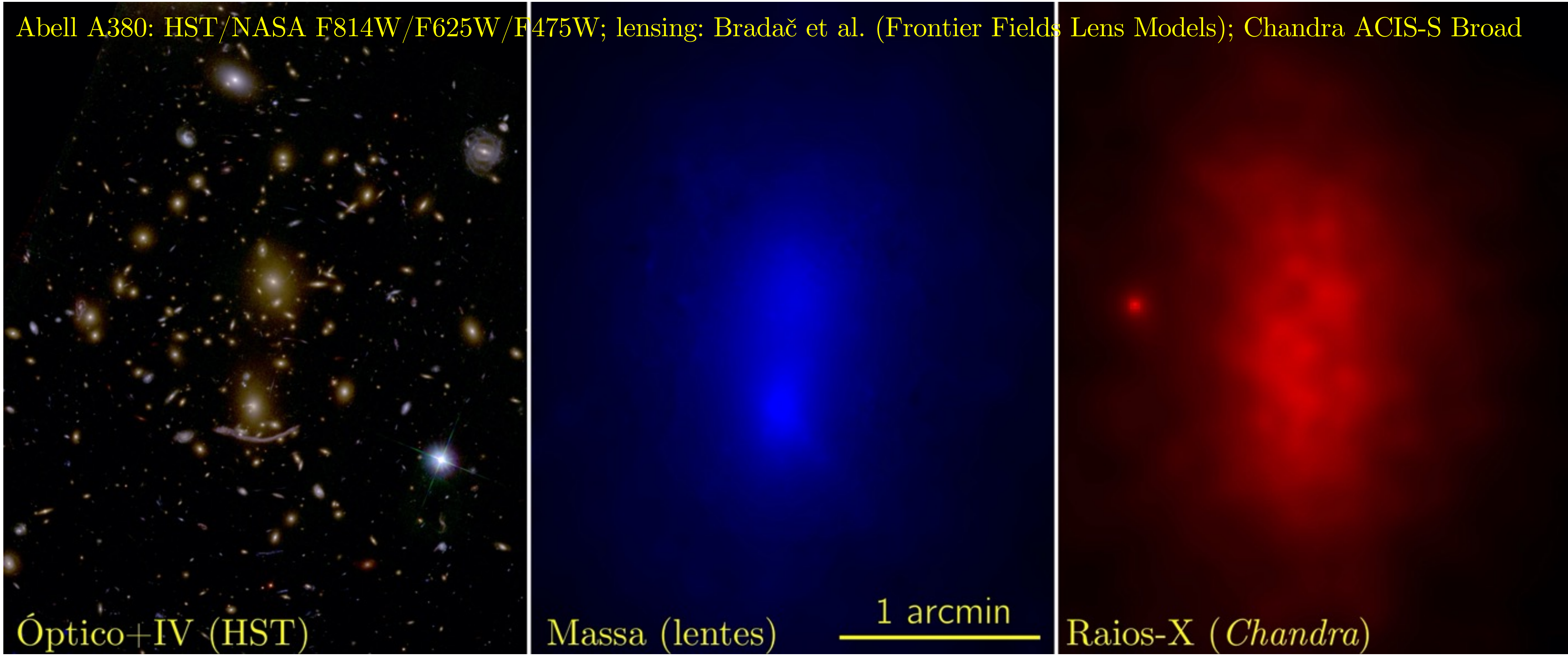

~ 3% stars (in galaxies and in the intracluster medium [diffuse light]);
~ 12% hot plasma (the intracluster gas);
~ 85% dark matter

These proportions (stars/hot plasma) change with the total halo mass

Baryonic mass fraction

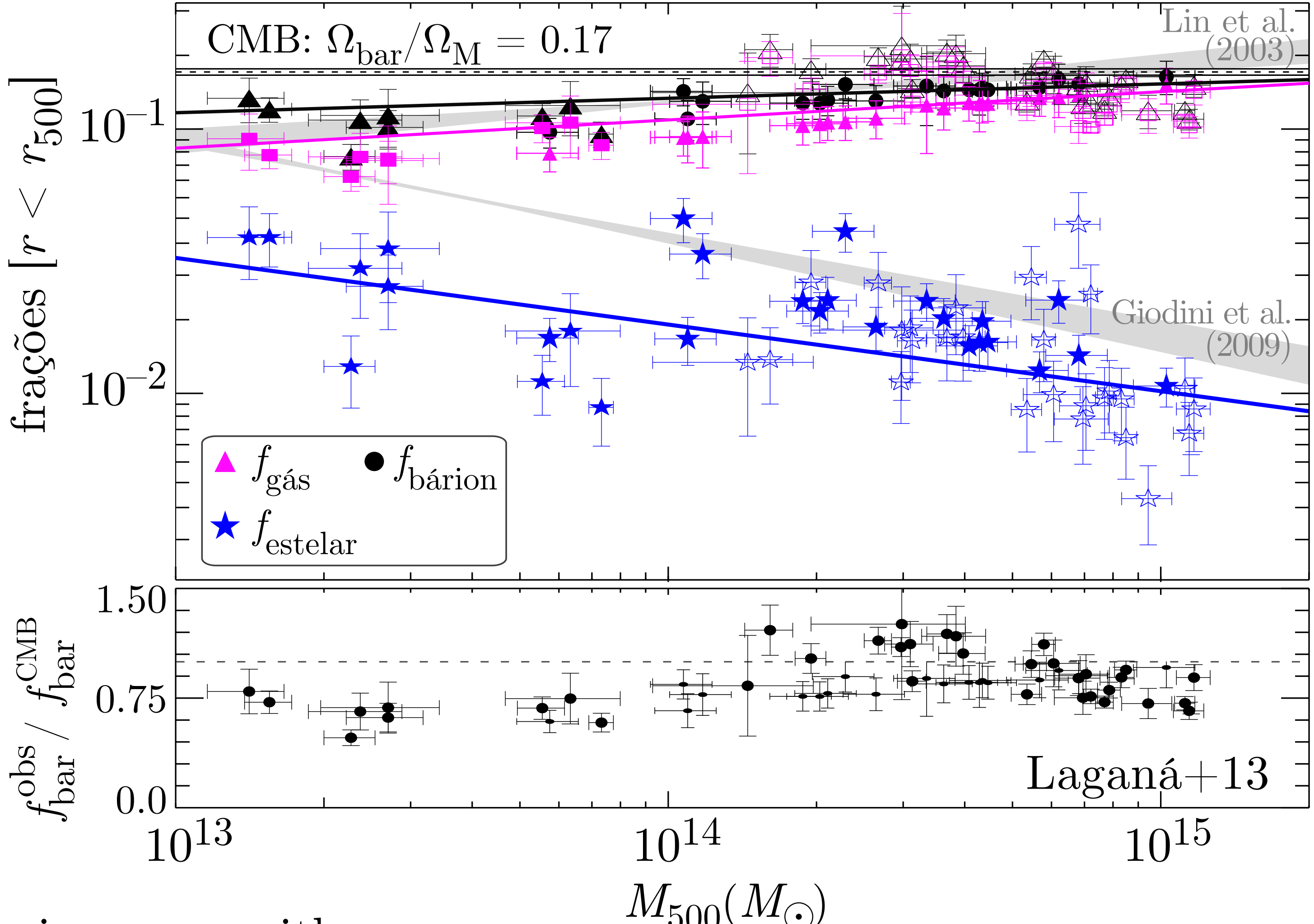

- Gas and baryon fractions increases with mass.
  - ✓ Also seen, by Gonzales+07; Giodini+09; Andreon+10; Laganá+13 (with somewhat different slopes)
- Fitting separately groups and clusters, different star fraction relations.
- The deficiency of baryons in groups (wrt WMAP/Planck) is greater in the center ($r < r_{2500}$): groups are not able to retain the gas in the center.

Galaxies in clusters

- Mainly early type (lenticulars and ellipticals).
  - ✓ Morphology segregation (Dressler 1980, 1997).

- Butcher-Oemler (1978, 1984) effect: galaxy population is bluer for higher redshift ($z \approx 0.5$).

- Evolutionary effects in high density environment.

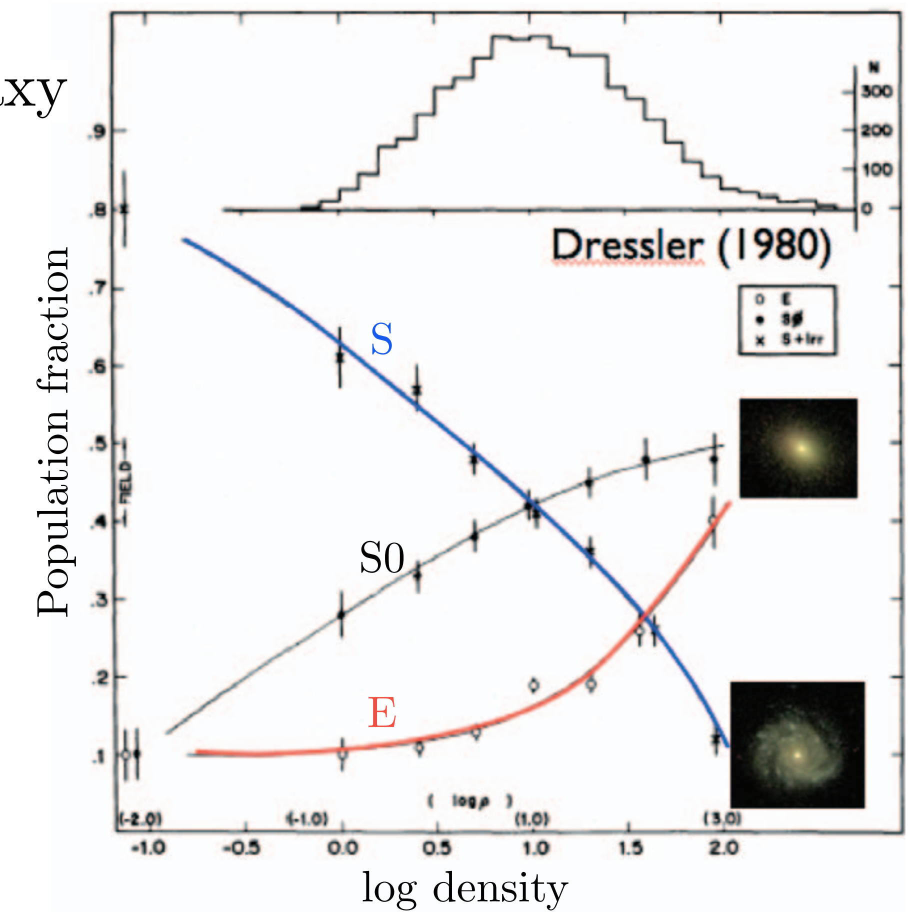

Red Sequence

- Early type galaxies **color-magnitude relation**, observed in clusters (Baum 1959; Faber 1973).
  ➔ More luminous E galaxies are redder

- Age or metallicity effect?
  - ✓ Semi-analytical models suggest **metallicity** is the main factor
  - ✓ More massive (luminous) galaxies keep the metal formed in stars.

- Useful method to detect clusters in photometric surveys (e.g. redMapper, Rykoff+2014).

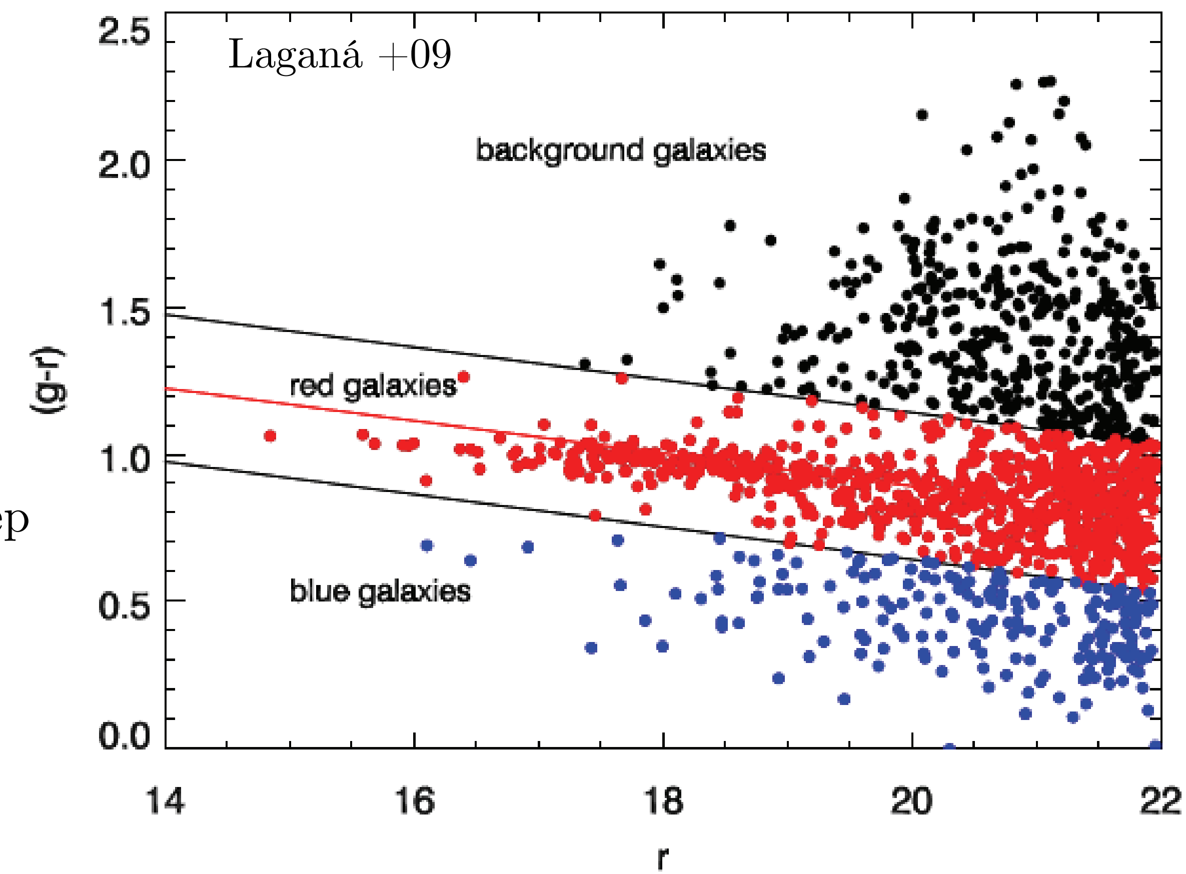

- Observation of high z galaxies with mature stellar population (red)
  ➔ small evolution of the red sequence.
  Galaxies with high stellar mass form stars quickly and intensly in the past, less massive galaxies take longer to form stars ➔ "downsizing", "preprocessing in groups"

Cluster--galaxy interaction

- Ram-pressure
  - ✓ cold interstellar gas striped by intracluster plasma (Gunn & Gott 1972).
- Strangulation/Starvation
  - ✓ hot coronae galactic gas striped by intracluster plasma (Bekki+ 2002).
- Tidal truncation
  - ✓ Galactic mass loss around virial radius stripped by cluster tidal forces (Fujita 1998).
- Harassment (not exactly cluster—galaxy, but occurs in clusters)
  - ✓ Galactic morphological perturbation/stripping of hot galactic atmosphere due to many close encounters (Moore+ 1998).
- Mergers (not exactly cluster—galaxy, but may occur in clusters)
  - ✓ Minor mergers X major mergers (Toomre & Toomre 1972)
  - ✓ Very important in low σ systems (groups).

Composition of galaxy clusters: observational evidences

- **Dark Matter**: $\approx 85\%$ in mass.
  - ✓ hydrostatic equilibrium (gas; X-ray): $\frac{1}{\rho}\nabla P = -\nabla\phi$
  - ✓ virial theorem (galaxies): $2K + U = 0$ (and Jeans equation)
  - ✓ gravitational lensing

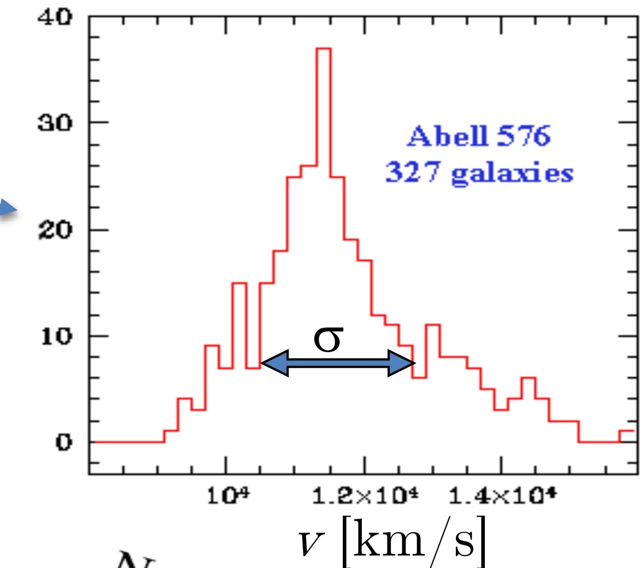

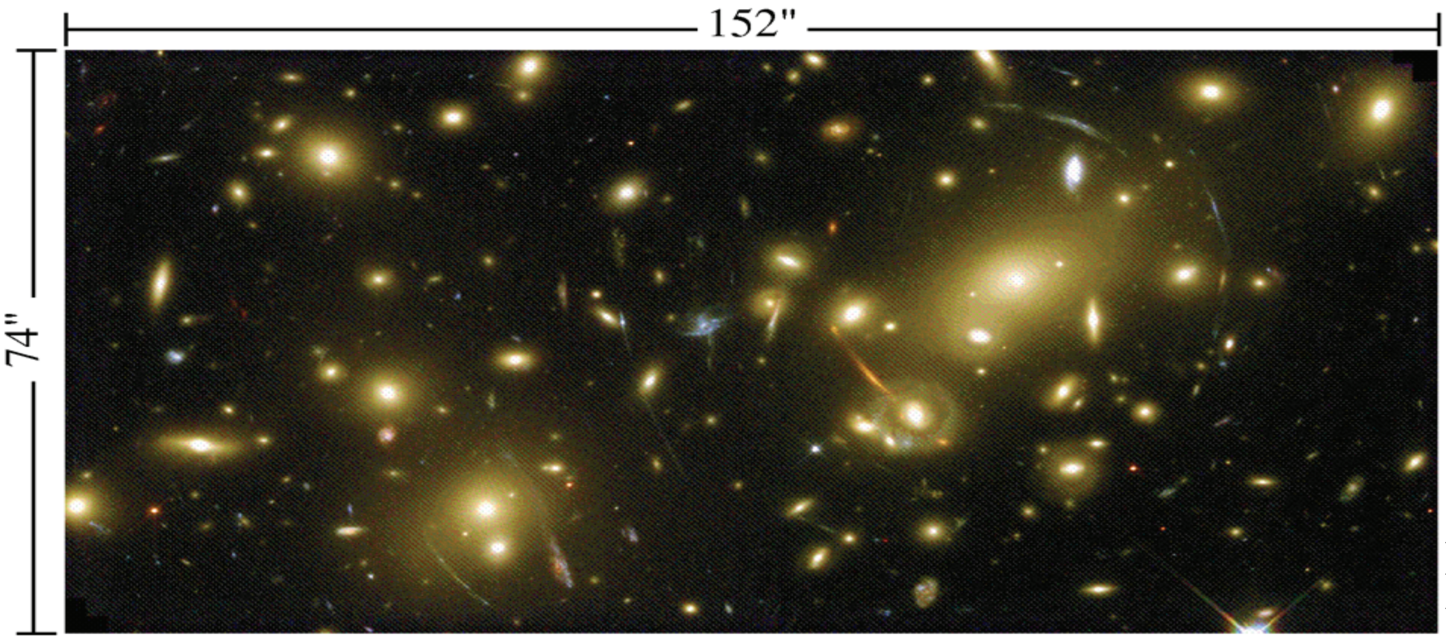

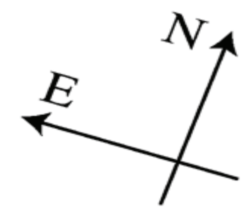

Abell 2218
HST

Composition of galaxy clusters

- **Intracluster gas**: $\approx 13\%$ in mass
  - ✓ X-ray emission
  - ✓ ram-pressure
  - ✓ SZ effect:

HI (galaxies) VLA

Intracluster gas (ROSAT)

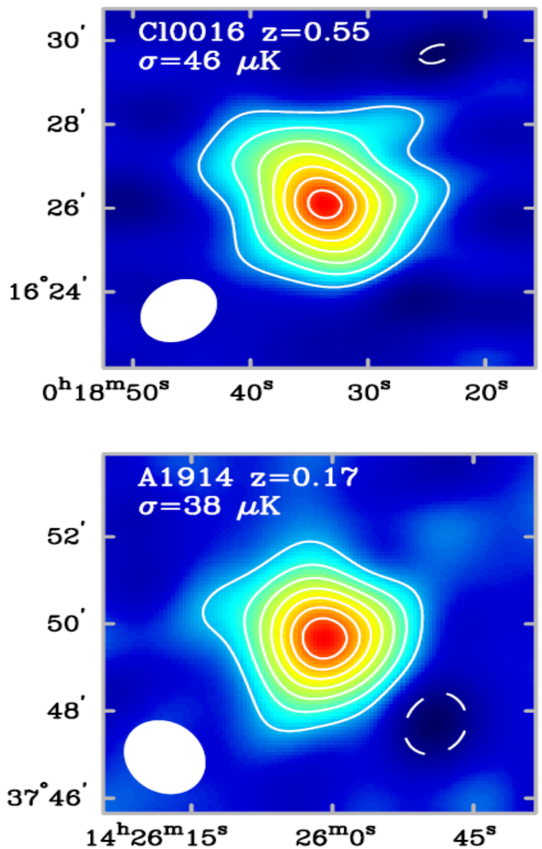

Reese 2003

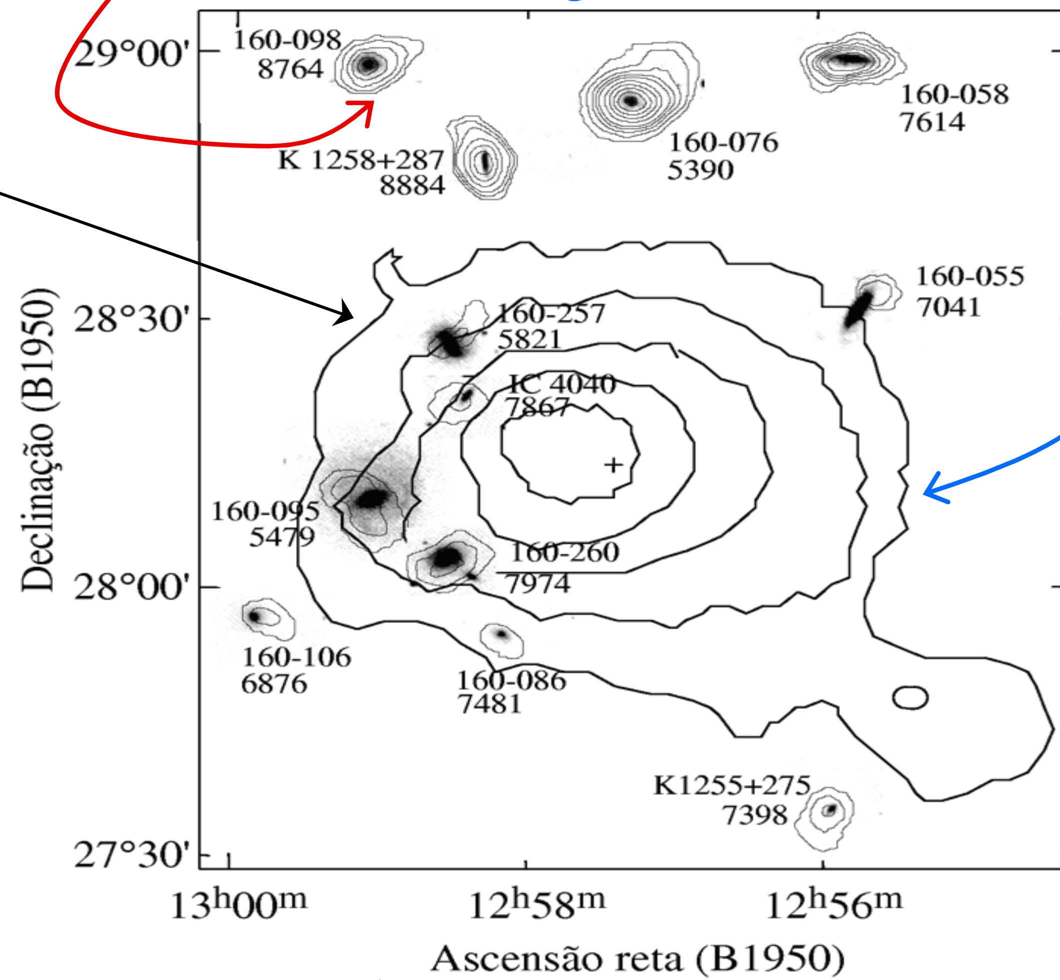

Coma Cluster

Bravo et al. 1999

Composition of galaxy clusters

- **Intracluster gas**: $\approx 13\%$ in mass
  - ✓ X-ray emission
  - ✓ ram-pressure
  - ✓ SZ effect:

Hydro/N-body simulation
(Ruggiero 2019)

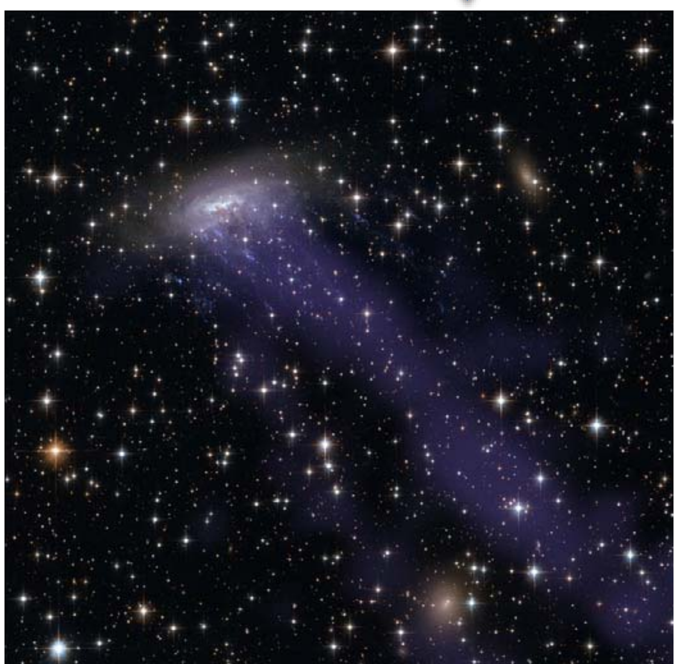

Jellyfish galaxies

ESO137-001 in cluster Abell 3627
HST+Chandra tail: Hα (near the galaxy) + X-ray
[actually 2 tails]

Sunyaev-Zel'dovich effect (radio/microwave)

- Inverse Compton scatter of CMB photons by ICM thermal free electrons ($kT \approx$ keV).

- Compton parameter: $$y = \frac{\sigma_T}{m_e c^2} \int kT(l)\, n_e(l)\, \mathrm{d}l$$ ← $n\,kT =$ pressure

- Apparent variation of CMB temperature: $$\frac{\Delta T_{\mathrm{CMB}}}{T_{\mathrm{CMB}}} = -2\,y$$
  - ✓ valid in the Rayleigh-Jeans low energy regime

- Modified blackbody spectrum
  - ✓ apparent decrease of temperature when measured in radio.
  - ✓ $\Delta T/T \approx 10^{-4} - 10^{-5}$. (same order of magnitude as the primordial temperature fluctuations)
  - ✓ At 217 GHz, the SZ effect is null.

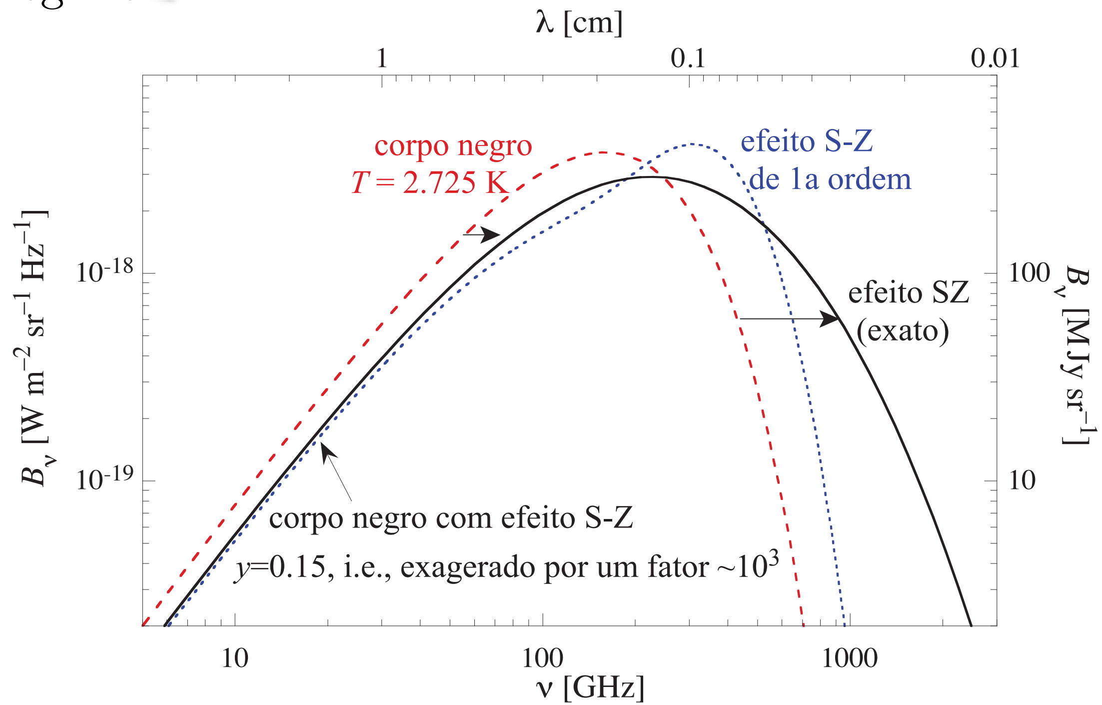

Sunyaev-Zel'dovich effect

- Search for cluster.
- First catalogues: *Planck* e SPT.
- Difficulties: spatial resolution, need several bands (confusion with other CMB fluctuations).

Planck SZ *catalogue*;
is the deepest all-sky.
0.1-1.6 10^{15} Mo.
$z < 1$.
1227 confirmed clusters.

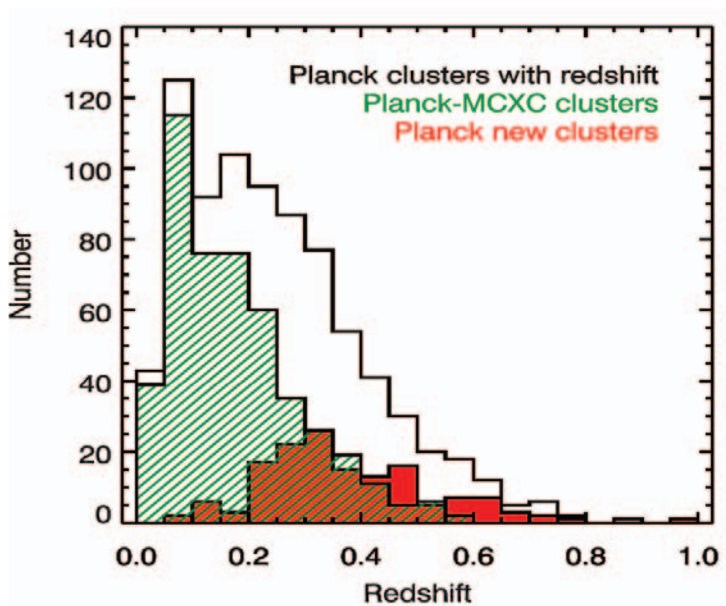

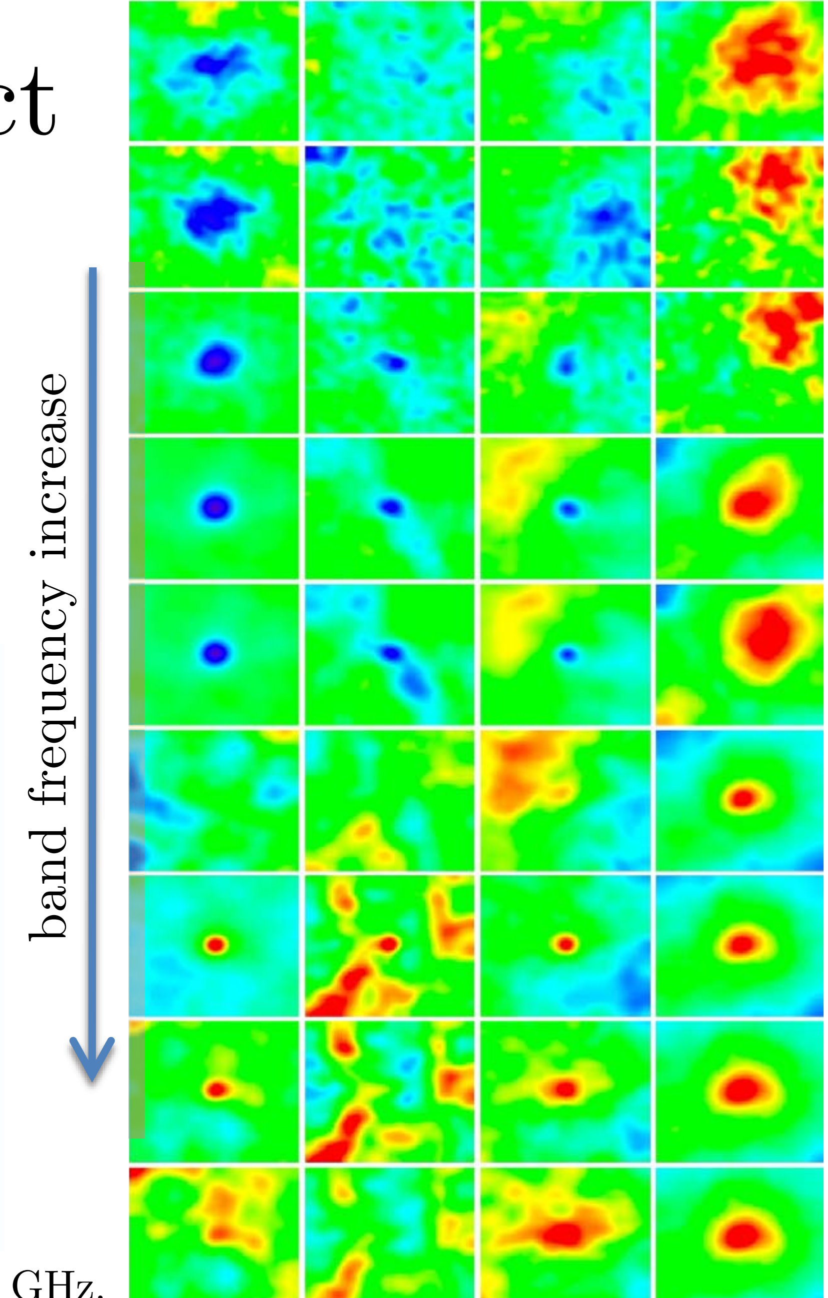

Images at Planck channels, from 30 to 857 GHz.
Planck Collaboration 2013, 2018

Sunyaev-Zel'dovich effect

- Signal does not depend on distance (redshift).
- Limited by spatial resolution (7′ *Planck;* 1′ SPT).
- Combining X-ray and SZ effect observations, distance indicator:

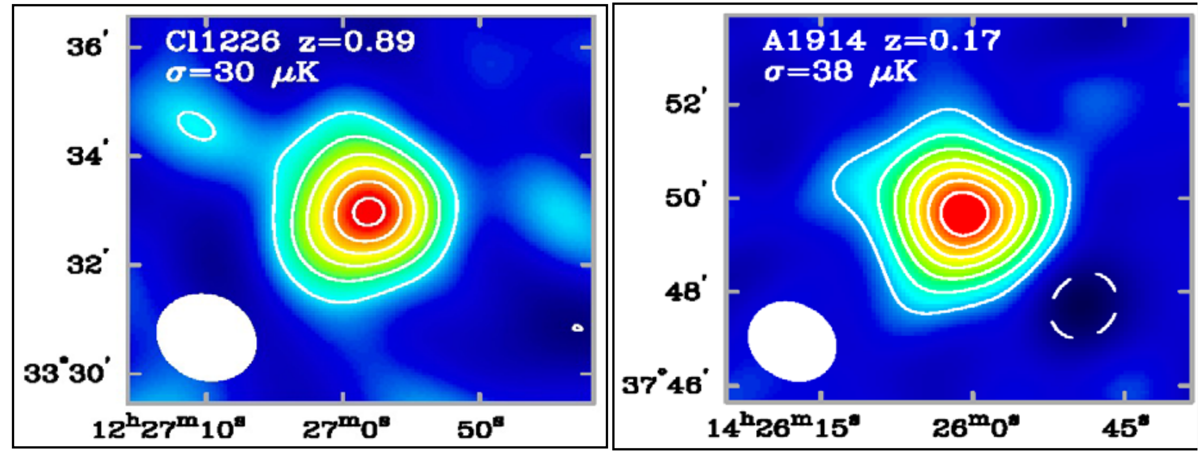

Temperature maps of CMB; note the difference in redshift.

$$\Delta T_{\mathrm{CMB}}/T_{\mathrm{CMB}} \propto \int n_e T_X \,\mathrm{d}l$$

$$L_X = 4\pi f_X d_L^2 \propto \int n_e^2 \Lambda(T_X)\,\mathrm{d}V$$

$$d_A \approx 4 \left(\frac{\Delta T/T}{10^{-5}}\right)^2_{\mathrm{CMB}} \left(\frac{f_X}{10^{-11}}\right)^{-1} \left(\frac{T_X}{10^8\mathrm{K}}\right)^{-3/2} \theta_c \;\; \mathrm{Mpc}$$

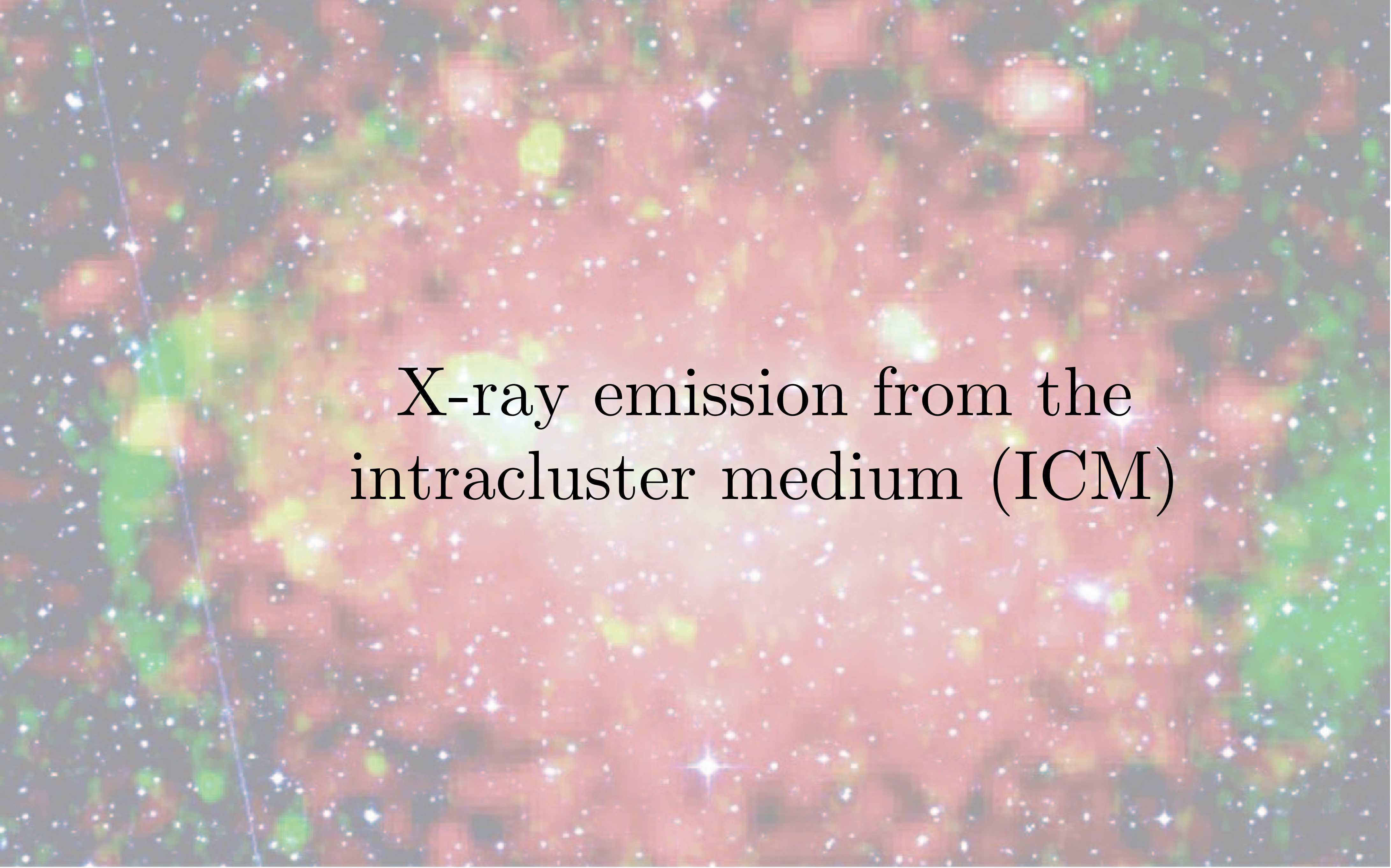

X-ray emission from the intracluster medium (ICM)

Bremsstrahlung continuum

- Thermal Bremsstrahlung :
  Optically thin plasma, colisional equilibrium.
  - ✓ hypothsis: Maxwell distribution of velocities (electrons and ions)
  - ✓ energy equipartition
  - ✓ electron – ion scatter
    (≈ 90% of ions are protons)

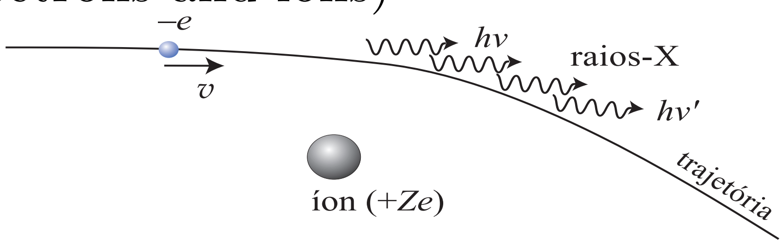

- $$\varepsilon_\nu \equiv \frac{\mathrm{d}E}{\mathrm{d}V\,\mathrm{d}t\,\mathrm{d}\nu} = 6{,}8 \times 10^{-38} Z^2 n_e n_i T^{-1/2} e^{-h\nu/kT} g(E,T) \ \text{erg s}^{-1}\text{cm}^{-3}\text{Hz}^{-1}$$

- For a primordial plasma (≈ 24% mass in He):

$$Z^2\, n_e n_i \approx 1.4\ n_e^2.$$

- $g(E,T)$ => Gaunt factor: relativistic and quantum corrections for scatter with small impact parameter and/or $E_{\mathrm{photon}} > kT$.
  - ✓ For clusters $g(E,T) \approx 1.0$–2.0

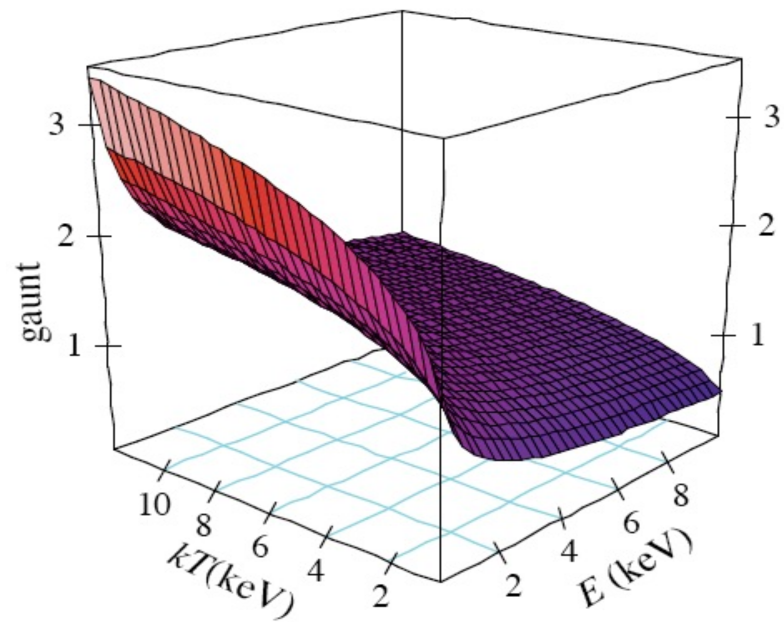

e.g., Rybicki & Lightman "Radiative Process in Astrophysics"

Gas cooling

- Cooling function, $\Lambda(T)$.
- Bremsstrahlung + line emission
- $\Lambda(T) = \varepsilon(T)/n^2$
- For only Bremsstralung:

$$\varepsilon \equiv \frac{\mathrm{d}E}{\mathrm{d}V\,\mathrm{d}t} = 1{,}426 \times 10^{-27} Z^2 n_e n_i T^{1/2} g(T) \ \ \mathrm{erg\ s^{-1}cm^{-3}}$$

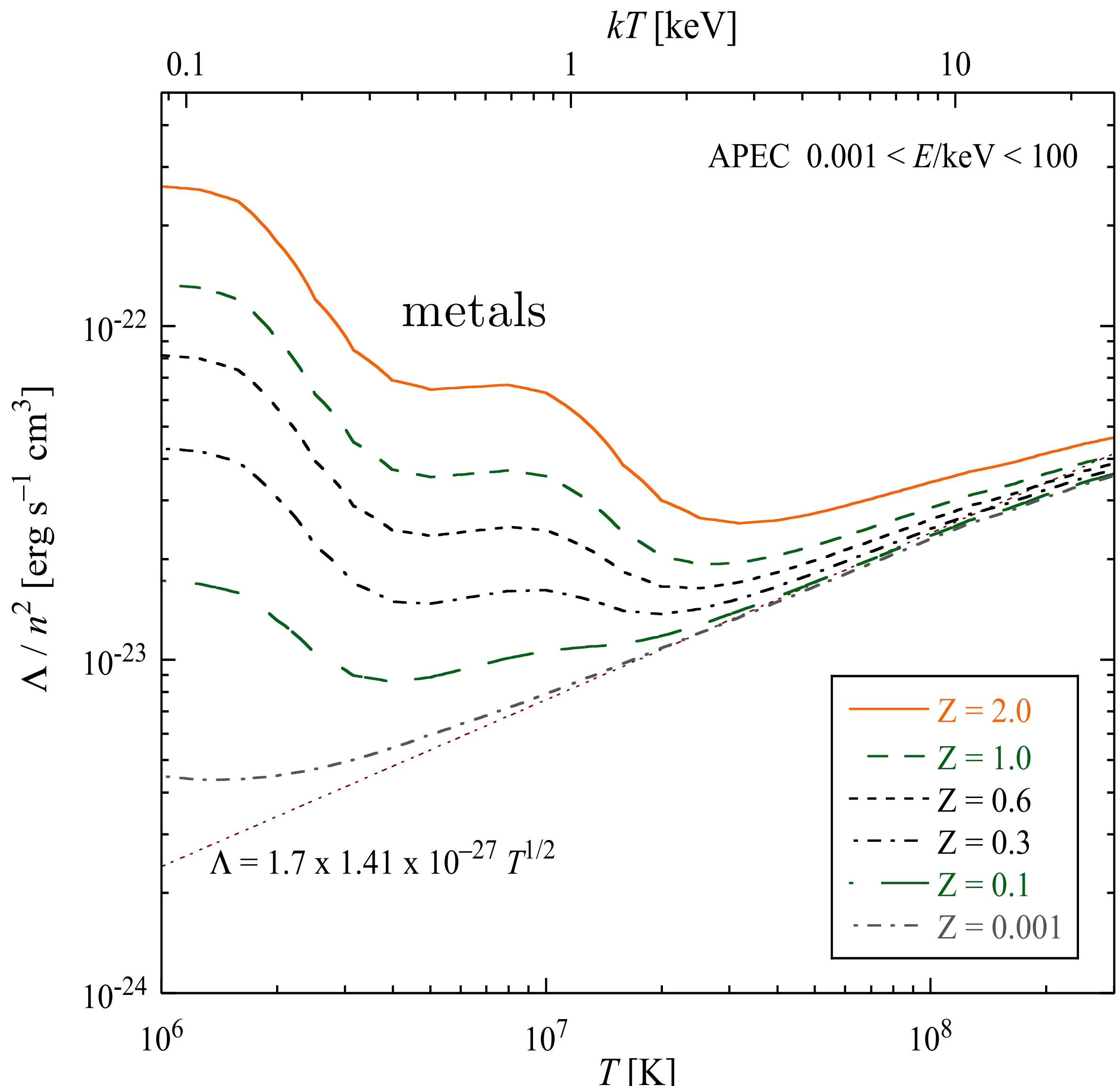

Intracluster plasma spectrum

- Absorption by neutral hydrogen in our galaxy for energy $E < 1–2$ keV.
  - ✓ $N_H \approx 10^{20}–10^{22}$ cm^{-2}.

- Exponential cut-off at $E \approx kT$.

- For $kT > 1,5$ keV, line complex Fe XXV e XXVI at $6,8/(1+z)$ keV.
  - ✓ K lines (decay to fundamental level).
  - ✓ Around $1.0/(1+z)$ keV, Fe L lines (decay to n=2 level).

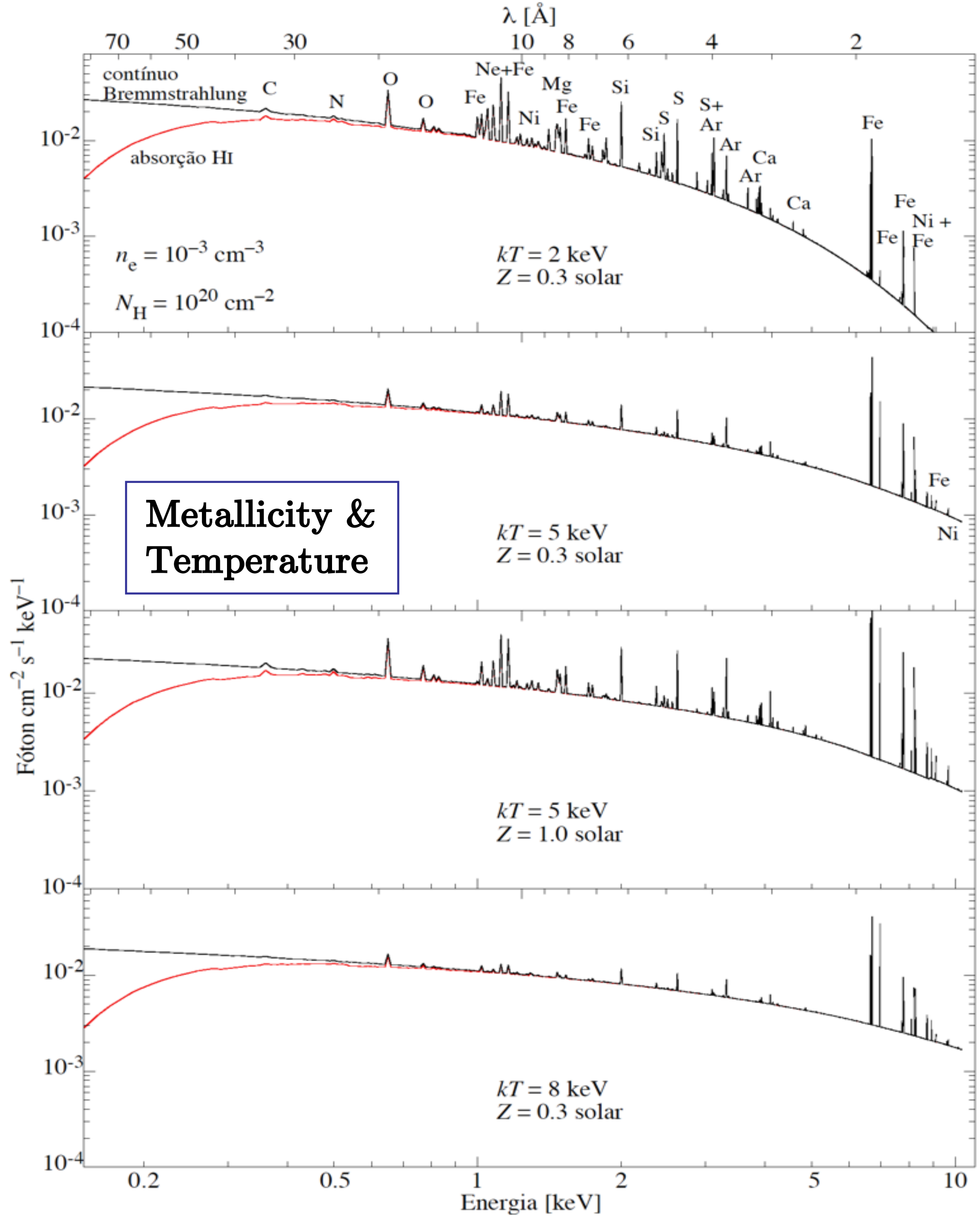

- We can determine some physical properties (e.g., density, temperature, metallicity) of the ICM from spectral fitting.

- Example: bright X-ray cluster ($\sim 10^{-12}$ erg/s/cm^2) observed by 100 ks (27h45m).

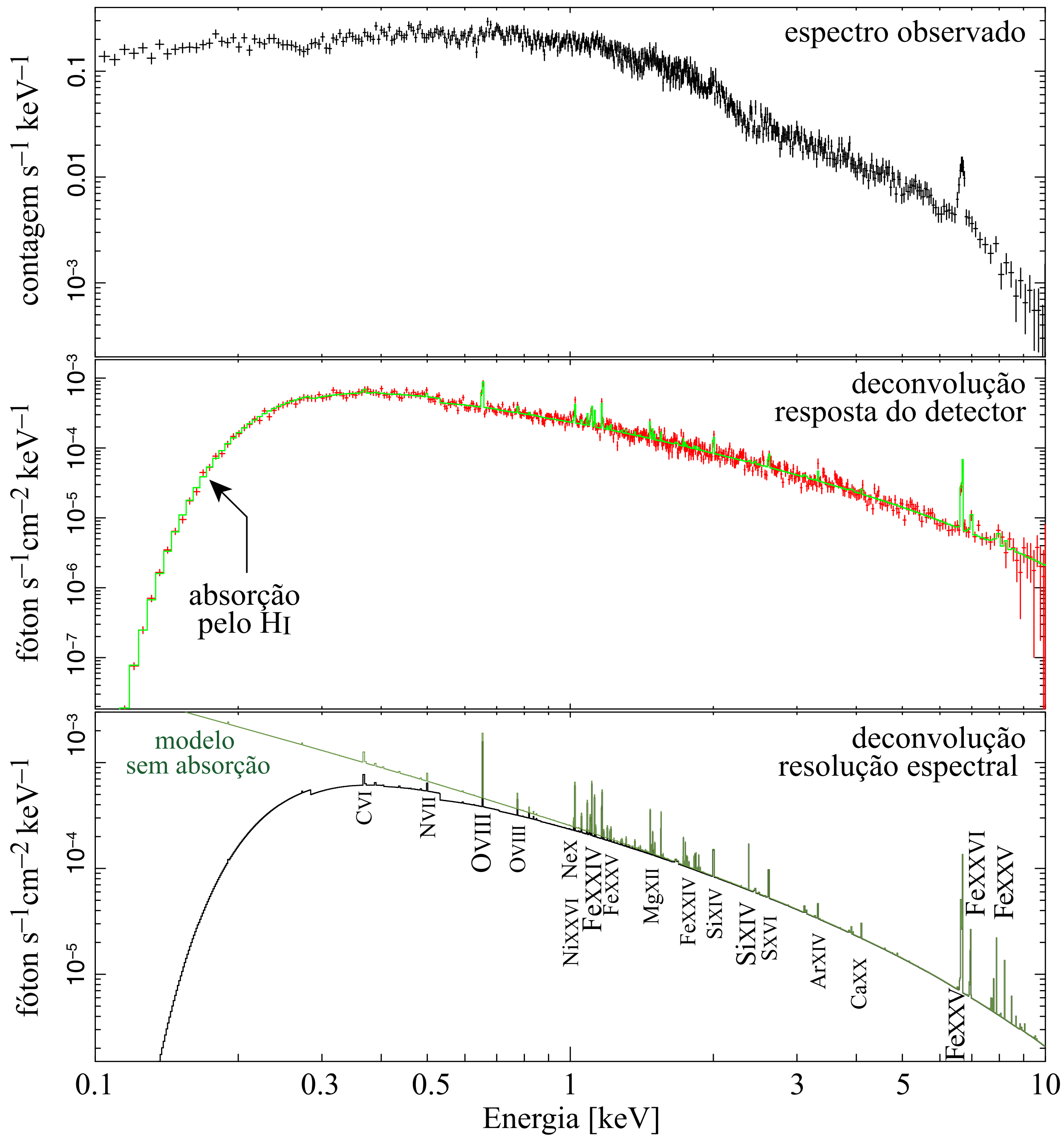

Cluster temperature comparison

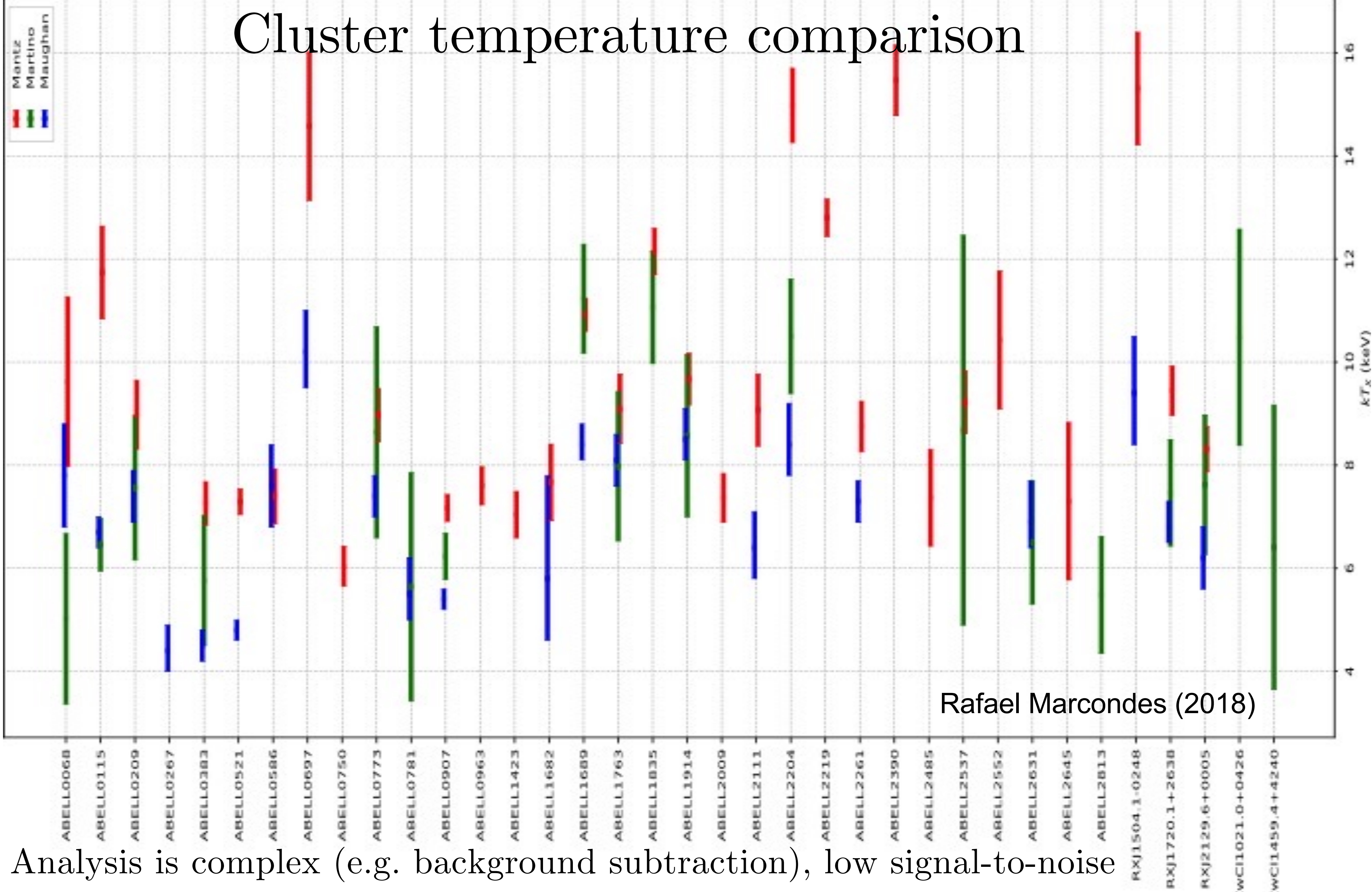

- Analysis is complex (e.g. background subtraction), low signal-to-noise

X-ray imaging

- Thermal bremsstrahlung emission integrated in energy (image):

$$\varepsilon \equiv \frac{\mathrm{d}E}{\mathrm{d}V\,\mathrm{d}t} = 1{,}426 \times 10^{-27} Z^2 n_e n_i T^{1/2} g(T) \ \ \mathrm{erg\ s^{-1} cm^{-3}}$$

  ✓ depends on n^2 and $T^{1/2}$ ==> gas image.

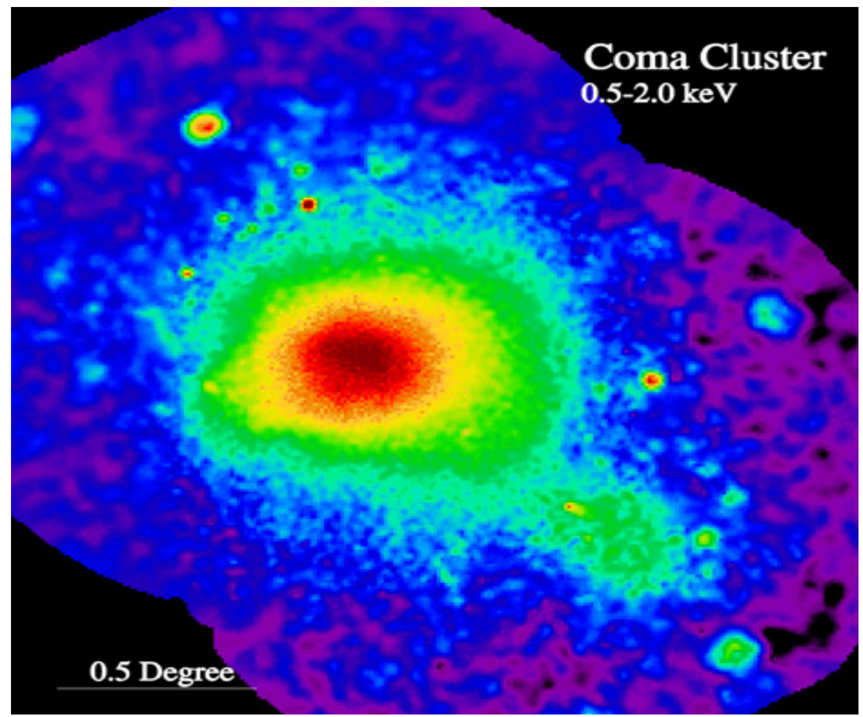

- Surface brightness radial profile:
  ✓ β-model (Cavaliere & Fusco-Femiano 1976):

$$\Sigma_X(R) = \Sigma_{X,0}\ \left[1 + (R/R_c)^2\right]^{-3\beta+1/2}$$

X-ray emission

- β-model is not always the best choice
  - ✓ cuspy emission in the center

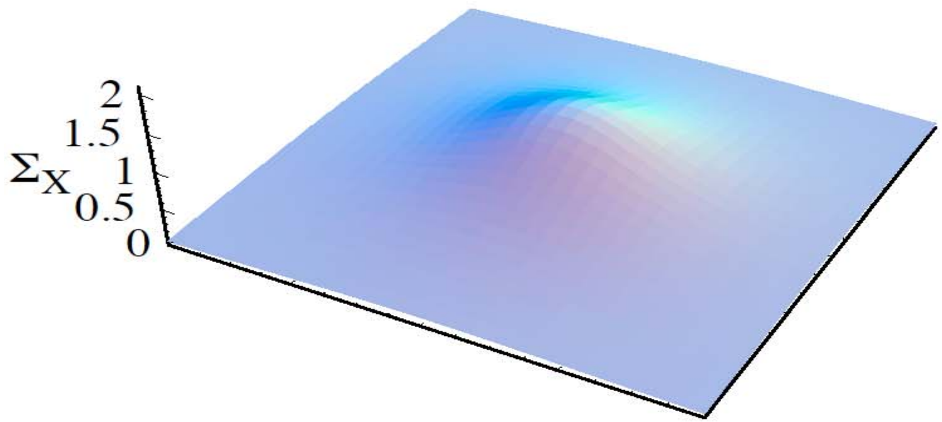

β-model

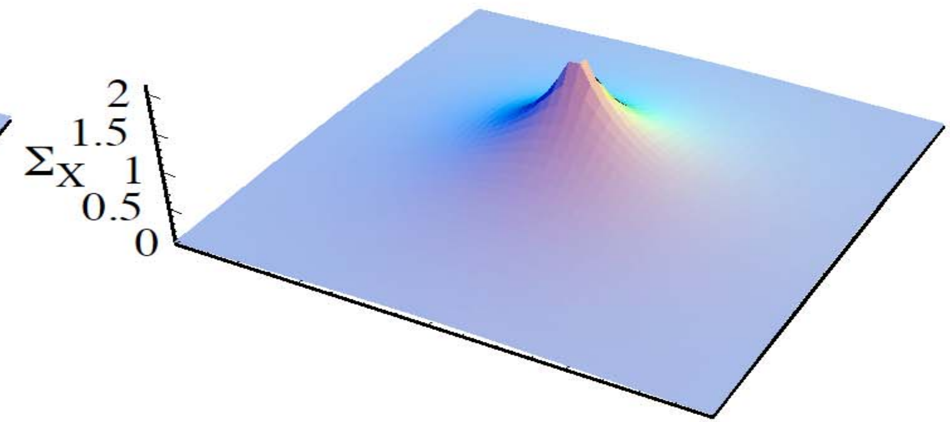

β-model + cusp

- Some other analytical radial profiles:
  - Sérsic (Demarco et al. A&A 2003), double-β-model (Xue & Wu, MNRAS, 2000), modified β-model (Maughan et al. ApJS 2008), etc.

Mass determination: hydrostatic

- Hydrostatic equilibrium: $$\frac{1}{\rho}\nabla P = -\nabla\Phi$$
- Spherical symmetry: $$\frac{1}{\rho(r)}\frac{\mathrm{d}P(r)}{\mathrm{d}r} = -\frac{\mathrm{d}\Phi(r)}{\mathrm{d}r}$$
- Hot gas ($\approx 10^7$ K), rarefied (10^{-3} cm^{-3}) ==> ideal gas.
  - ✓ $P = n\,kT + P_{\rm nt}$. We have also $\rho = n\,\mu\,m_{\rm H}$.
- Gravitational potential gradient: $$\frac{\mathrm{d}\Phi}{\mathrm{d}r} = -F(r) = \frac{G\,M(r)}{r^2}$$
- Therefore, $$\frac{1}{\rho}\left[\frac{k}{\mu m_{\rm H}}\frac{\mathrm{d}(\rho \mathrm{T})}{\mathrm{dr}} + \frac{\mathrm{dP_{nt}}}{\mathrm{dr}}\right] = -\frac{\mathrm{d}\Phi(\mathrm{r})}{\mathrm{dr}} = -\frac{GM(r)}{r^2}$$

Mass determination: hydrostatic

- Hydrostatic equilibrium, spherical symmetry:

$$M(r) = -\frac{kT}{G\,\mu\,m_{\rm H}}\,r\left(\frac{{\rm d}\ln\rho}{{\rm d}\ln r} + \frac{{\rm d}\ln T}{{\rm d}\ln r} + \frac{P_{\rm nt}}{P_{\rm th}}\frac{{\rm d}\ln P_{\rm nt}}{{\rm d}\ln r}\right)$$

$P_{\rm nt}$ = non-thermal pression

total mass or dynamical mass

gas density and temperature

- ✓ Gas density radial profile determined with the X-ray SB emission (image).
- ✓ Temperature profile determined using spatial resolved spectroscopy.
- ✓ Very strong evidence of large amount of dark matter.

Surface brightness

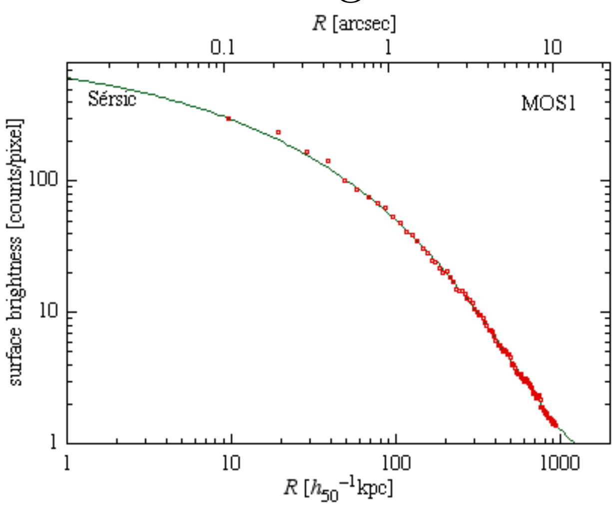

Dynamical mass (density)

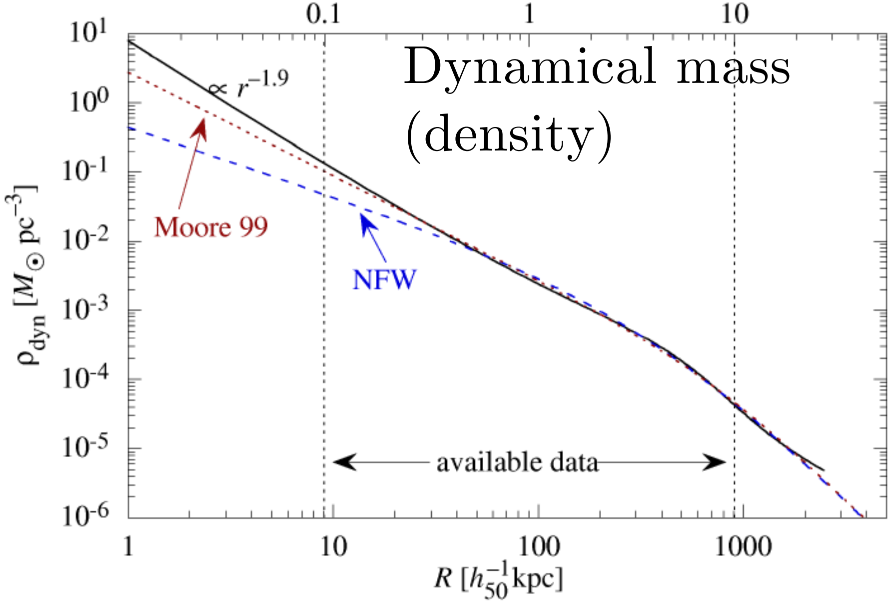

Temperature

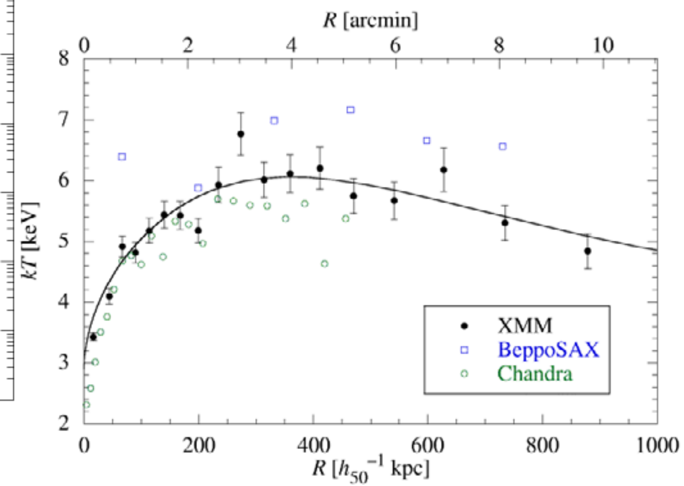

Cooling-flow

- X-ray emission → energy loss (mainly bremsstralung).
  - ✓ Cooling time scale: $E/(\mathrm{d}E/\mathrm{d}t)$,
    where $E = (3/2)\ n\ kT$ is the gas energy and $\mathrm{d}E/\mathrm{d}t = L_\mathrm{X}$.

$$t_\mathrm{cf} \simeq 9.3 \times 10^9 \frac{(kT_\mathrm{kev})^{1/2}}{n_3}\ \mathrm{yr}$$

(some authors prefer to use the entalpy, $(5/3)\ n\ kT$)

- Prediction: in the center, where the density is higher, the cooling time is smaller than the age of the cluster. Therefore, the gas should cool completely.

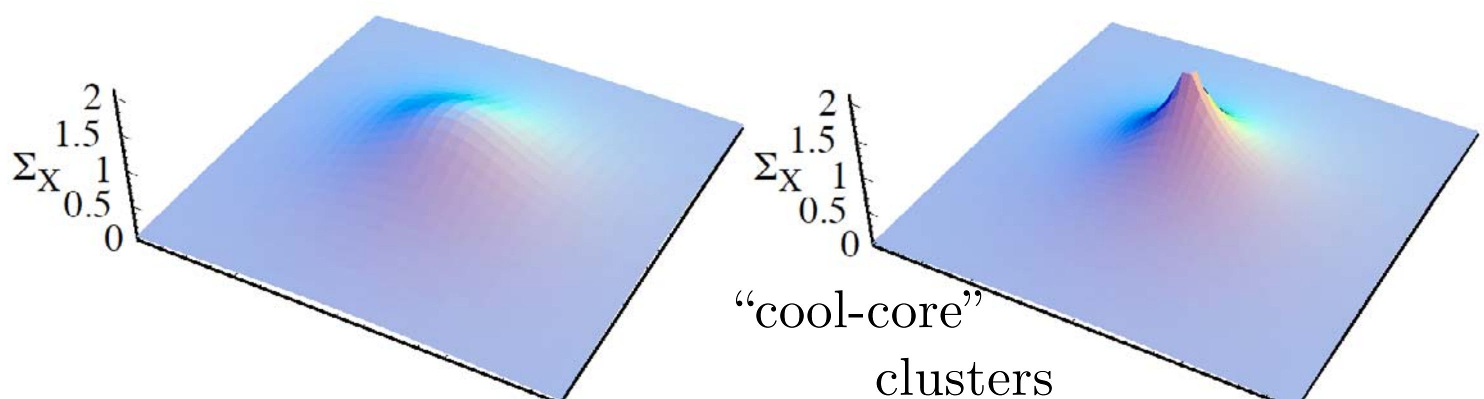

“cool-core” clusters

Cooling-flow

- Cooling time as a function of the cluster radius

- Inside 100–200 kpc, the gas should cool withing a Hubble time.

- The gas should accumulate in the center, 100s of solar mass per year.
  → Total mass deposit around 10^{12} $M_\odot$.

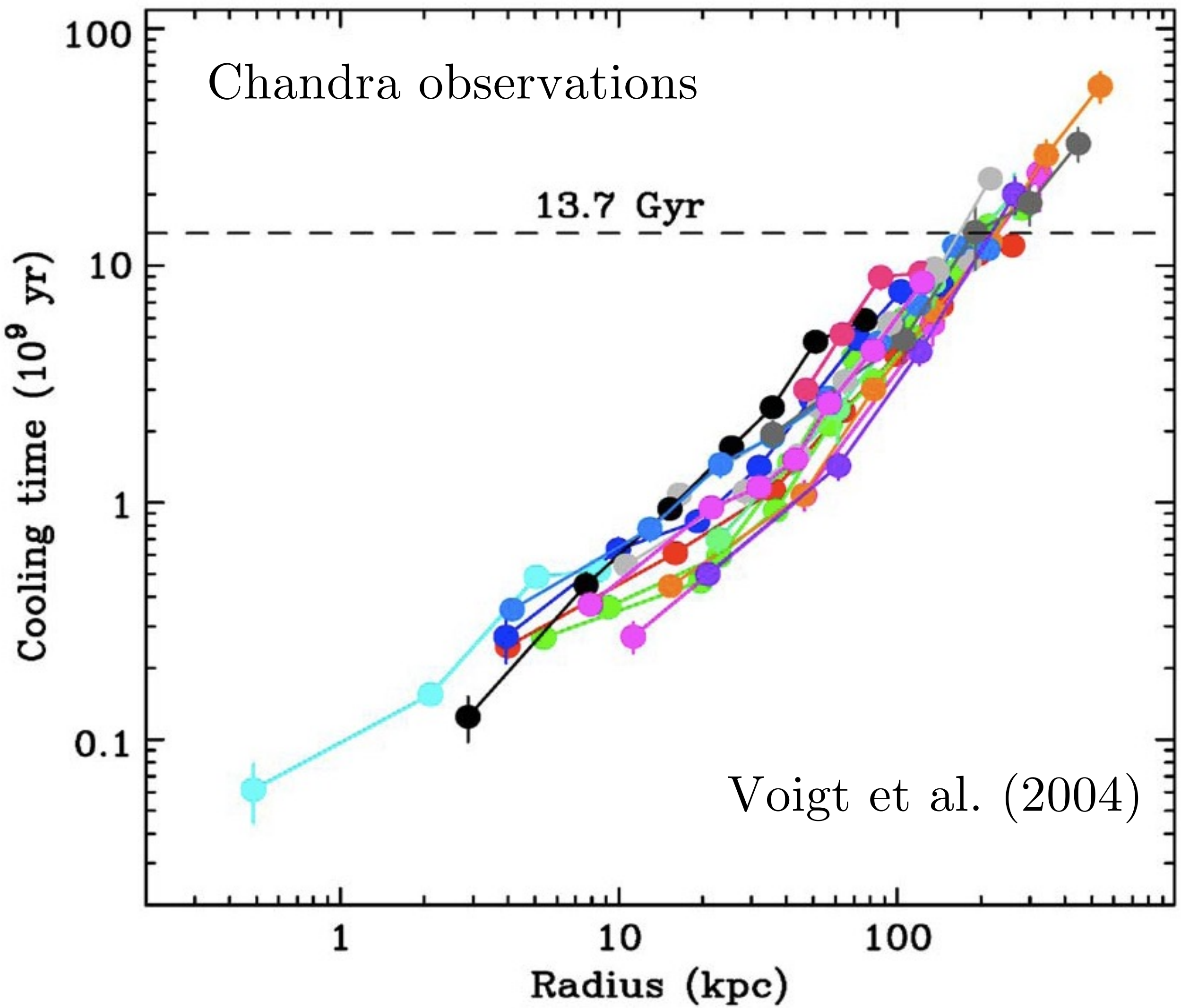

Cool-core

- High gas mass deposit rate is not observed.
- Since 2001, it is observed a lack of cold gas in the center.
  - ✓ XMM-*Newton* observations Peterson et al. 2001, 2003:

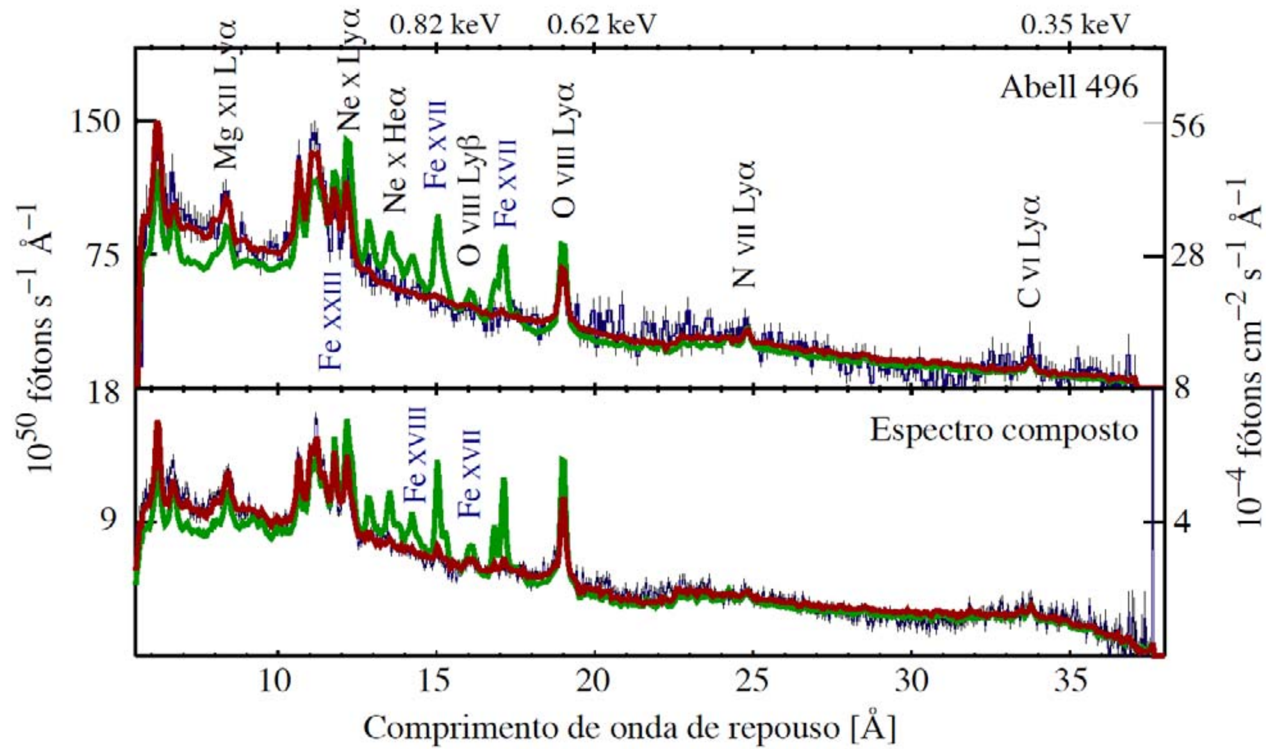

- What mechanism could head the gas in the center?
  - ✓ AGN, SNs, thermal conduction, merging clusters (shock)...
  - ✓ Some feedback mechanism? (central temperature ≈ (1/3) virial temperatuea).

Temperature profile

- Temperature drop in the center.
- In cool-core clusters $T_{\rm central} \approx T_{\rm virial}/3$
- Slowly decrease for $r > 0.2\ r_{\rm vir}$.
- Dificult to measure the gas temperature at $r \approx r_{\rm vir}$.

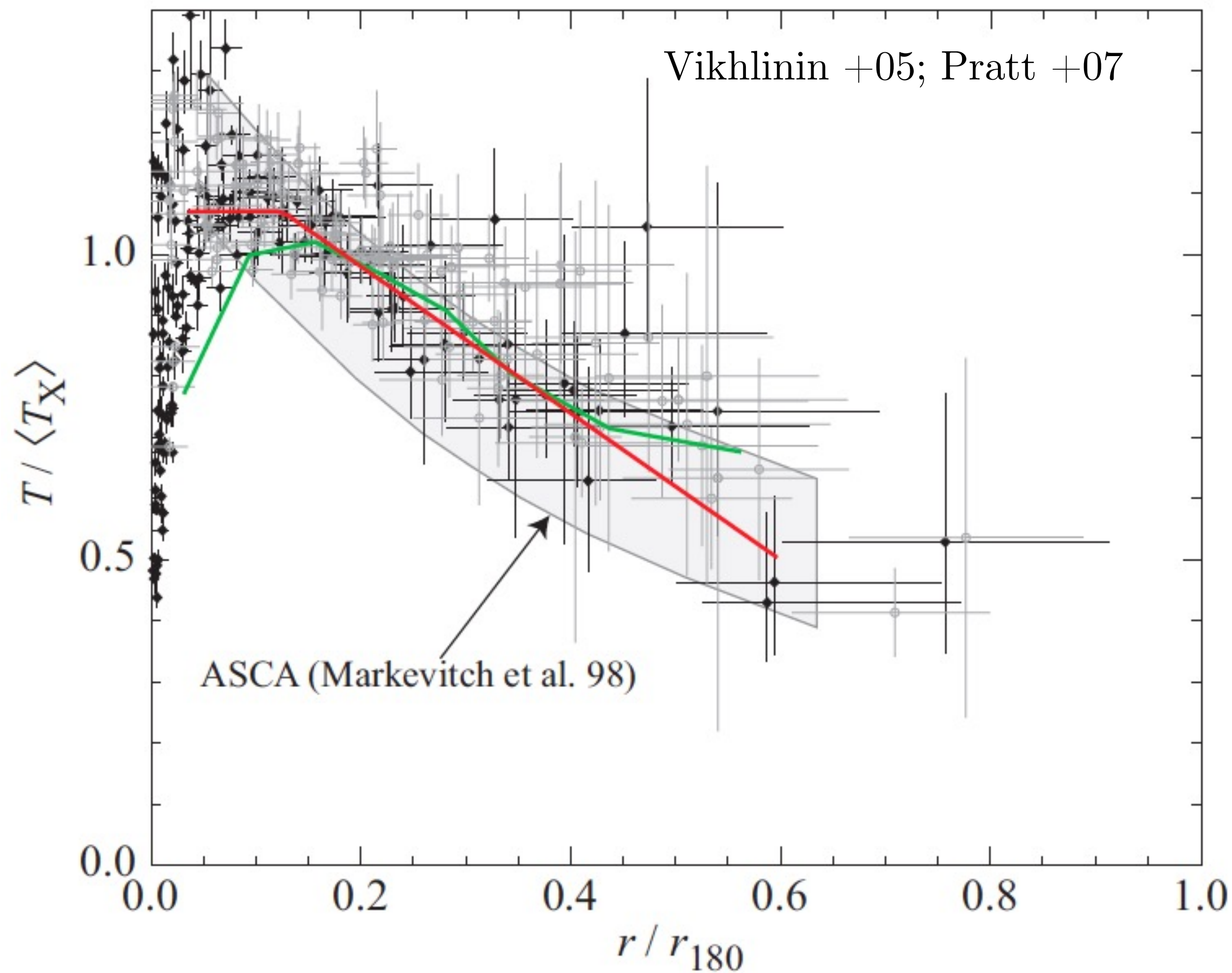

Radio jets ICM interaction

Optical image
DESI *grz*.

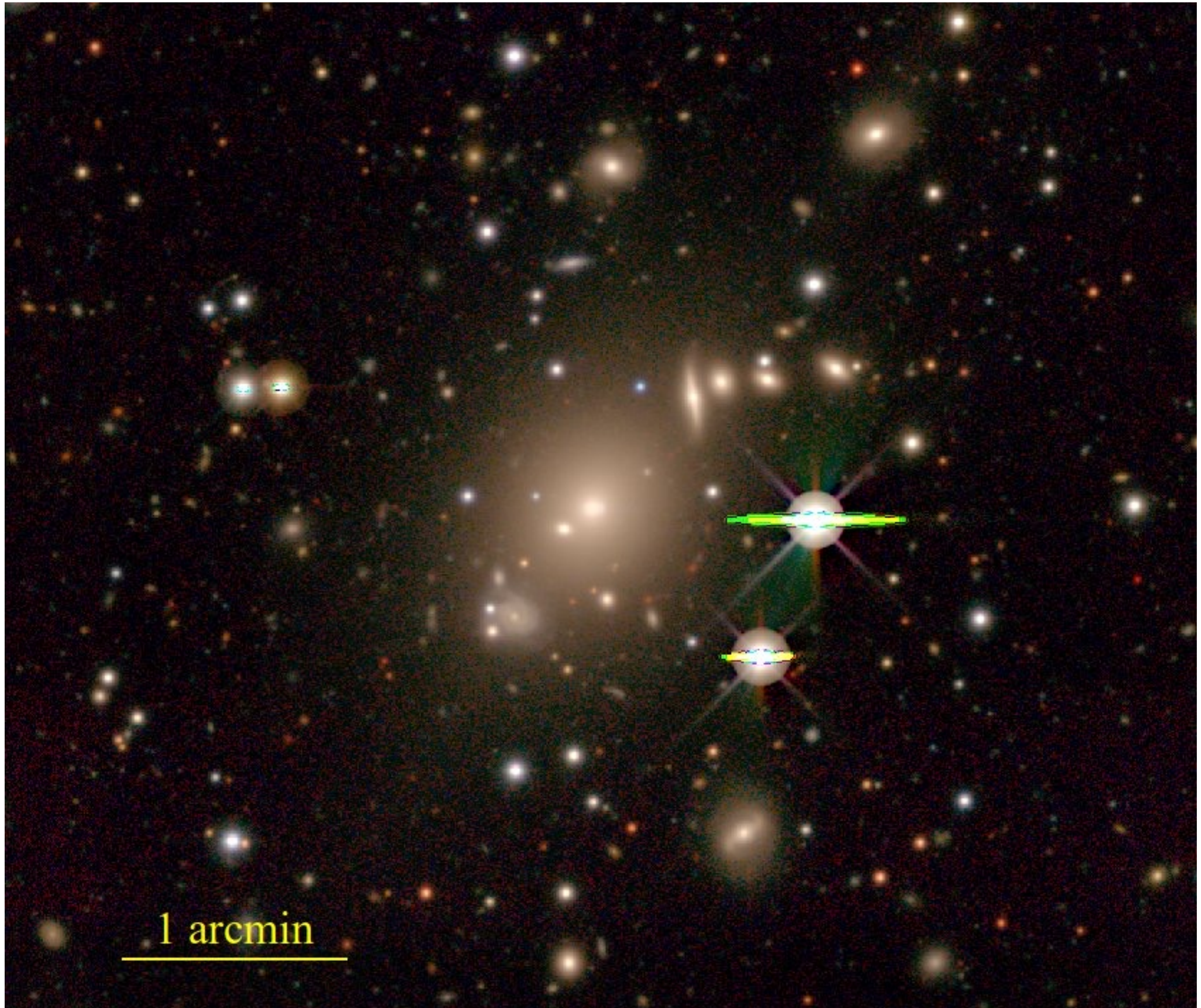

Hydra A Cluster
(Abell 780)

Radio jets ICM interaction

X-ray image
Chandra
[0.3–8.0 keV]

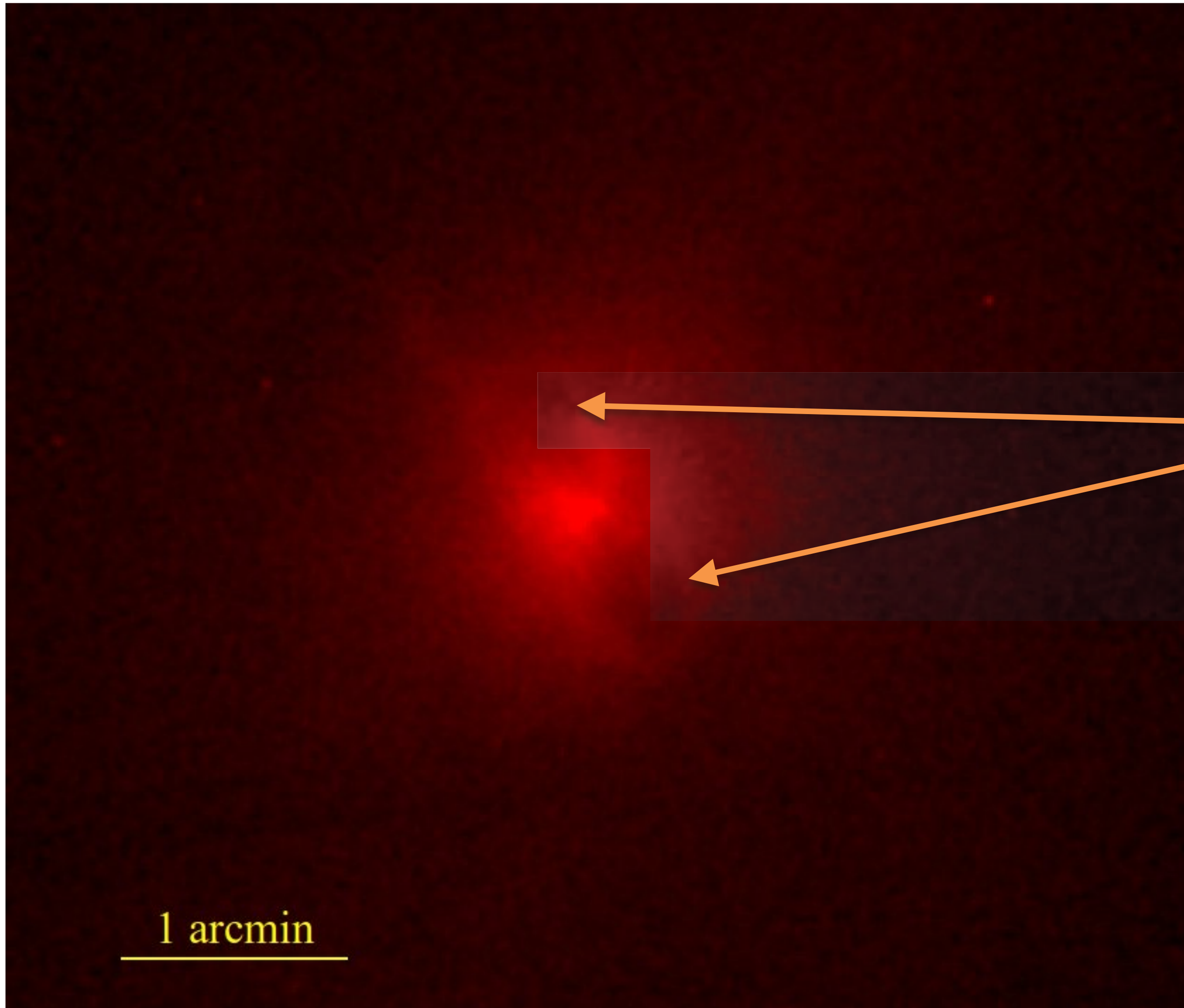

"Bubbles"

Hydra A Cluster
(Abell 780)

Radio jets ICM interaction

Radio image
VLA
[4.6 GHz]

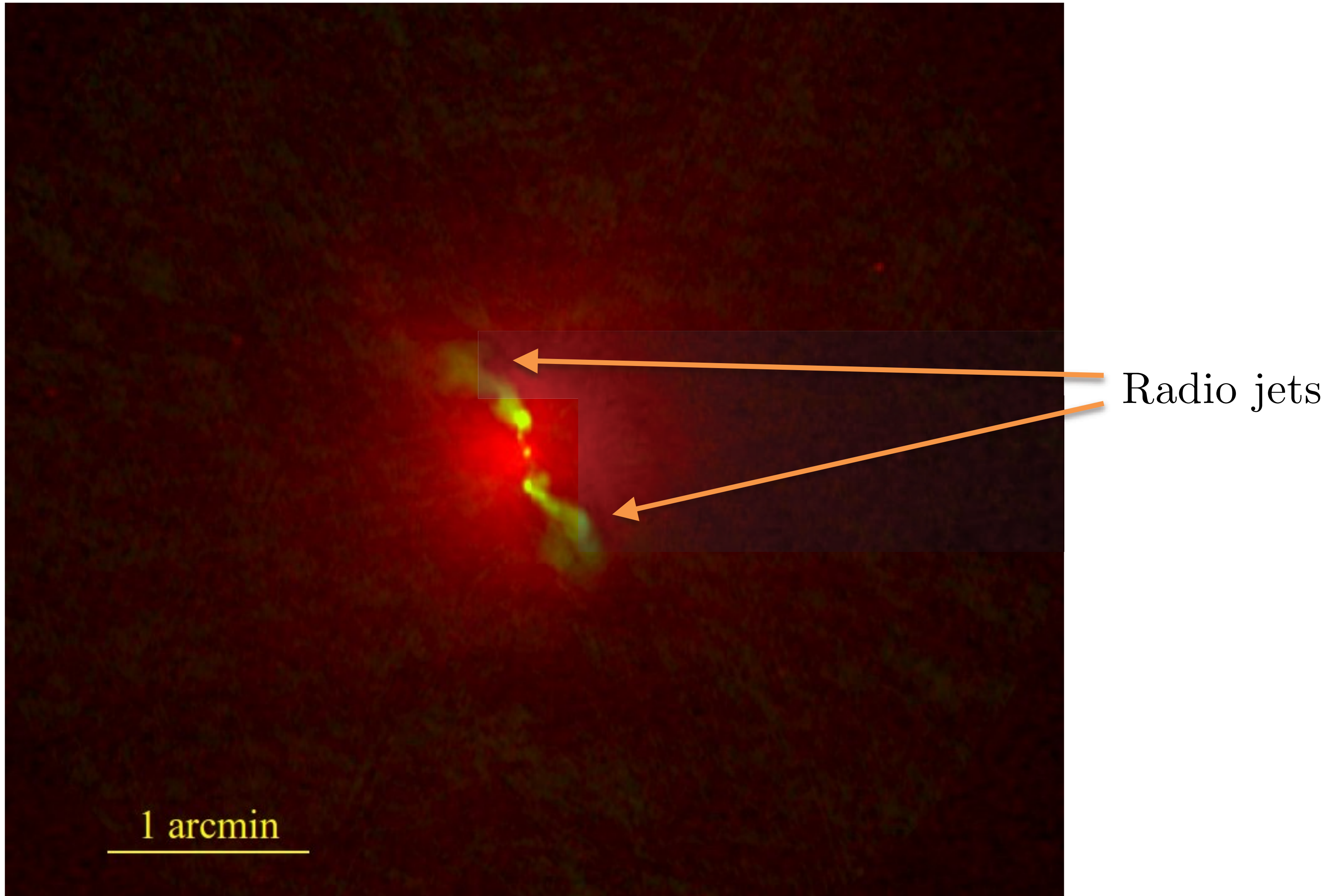

Hydra A Cluster
(Abell 780)

Thermal gas equilibrium in clusters

- Evidences:
  - Gas structure (morphology)
  - Radial temperature profile: floor at the center $\approx T_{\mathrm{vir}}/3$

- Colling-flow feedback:

  - Energy loss: X-ray emission (bremsstrahlung).
  - Central matter infall: pressure radial gradient.
  - AGN activates (increases), relativistic particle ejection: radio jets.
  - Gas heating, cooling-flow quenched.
  - AGN stops being fed by infalling gas.
  - Gas starts cooling again, density rises increase energy loss → infall restarts.

Blanton et al., 2010, PNAS; Fabian 2012, ARA&A; Rasia et al. 2015 ApJ;
Hlavacek-Larrondo et al, 2022, in "Galaxy Clusters"; Ubertosi et al. 2023 A&A

Scaling relations

- Linking physical properties in simple relations
  - ✓ Useful as proxies of cluster masses.
  - ✓ May reveal evolutionary properties or physical processes acting on clusters when compared to simple models
- Example:

$$L_X \propto \int \varepsilon \, \mathrm{d}E \, \mathrm{d}V \Rightarrow L_X \propto \rho_0^2 R_c^3 T^{1/2}$$

$$M_g \propto \int \rho \, \mathrm{d}V \Rightarrow M_g \propto \rho_0 R_c^3$$

$$M_d = \frac{kT}{G\,\mu\,m_p} r \left(-\frac{\mathrm{d}\log\rho}{\mathrm{d}\log r} - \frac{\mathrm{d}\log T}{\mathrm{d}\log r} \right) \Rightarrow M_d \propto R_c T$$

$$f = \frac{M_g}{M_d} \Rightarrow f \propto \rho_0 R_c^2 T^{-1}$$

✓ suposing $f =$ constant: $\rho_0 \propto R_c^{-2} T$

✓ suposing $M_\mathrm{d} \propto R_\mathrm{c}^3$ (same density): $R_c \propto T^{1/2}$

✓ So: $L_x \propto T^2$ e $M_g \propto T^{3/2}$

[For grups and clusters, R_{vir} is about R_{200} that is defined by the halo density 200x larger than the mean density of the Universe.]

Scaling relations

- $L_X \propto T^2$ and $M_{gas} \propto T^{3/2}$

  $T_X \propto \sigma^2$ and $L_X \propto \sigma^4$

- These are not exactly as the observed relations.

Clusters	$L_X \propto T^{2,79}$	$L_X \propto \sigma^{5,30}$	$\sigma \propto T^{0,65}$
Groups	$L_X \propto T^{5,57}$	$L_X \propto \sigma^{2,35}$	$\sigma \propto T^{0,64}$

- Non-gravitational process at play:
  - ✓ Preheating
  - ✓ SNs
  - ✓ AGN

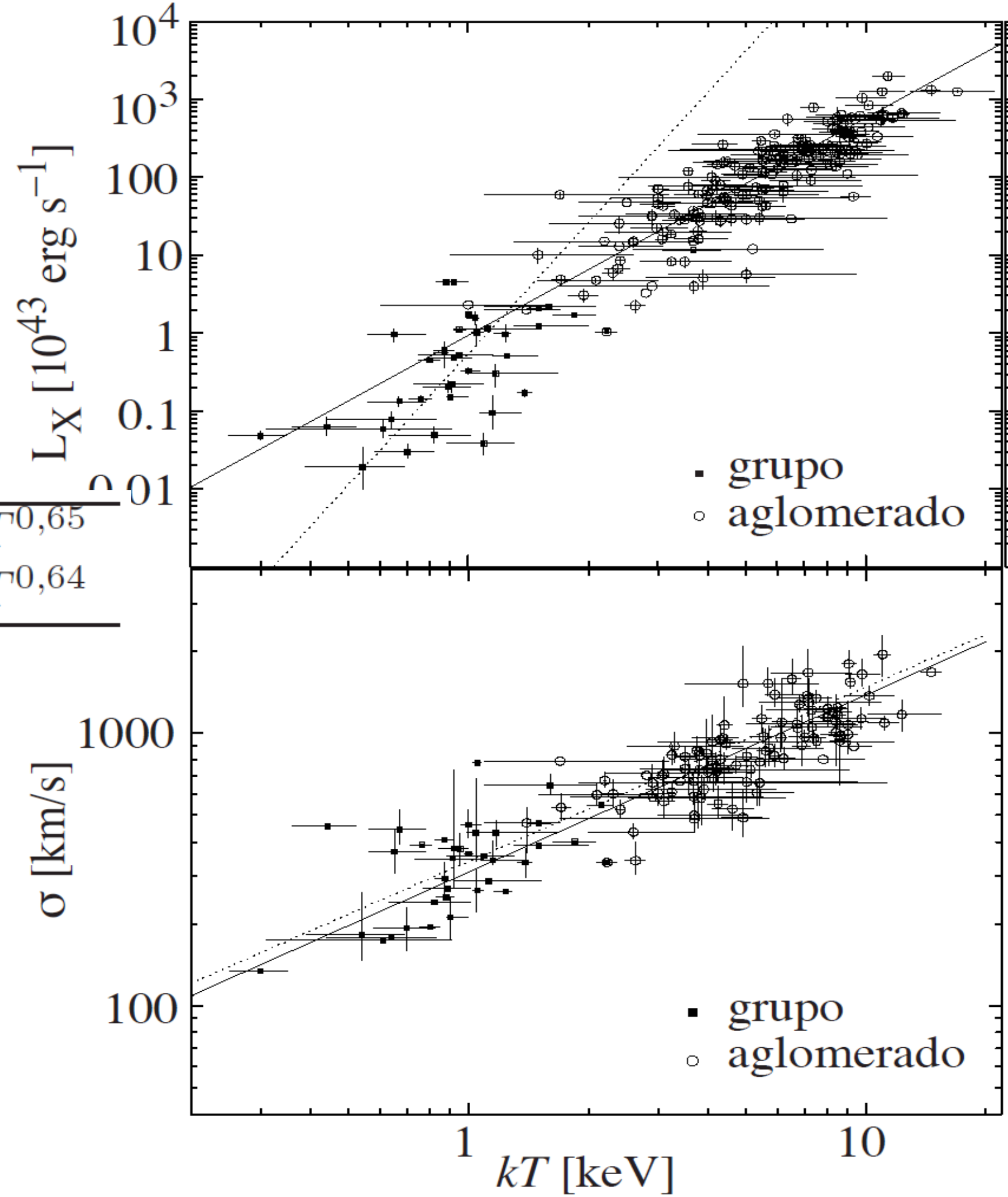

Scale relations

- Kravtsov et al. (2006) introduced $Y = M_{\rm gas}\, kT$, related to the energy of the ICM.
- It's related to the SZ effect: $Y_{SZ} = \dfrac{k\sigma_T}{m_e c^2} \displaystyle\int T\, n_e\, {\rm d}V \propto M_{g\acute{a}s} T$
- Using the following scaling: $M_d \propto R_c T$ e $R_C \propto T^{1/2} \Rightarrow M_d \propto T^{3/2}$ and $\mathcal{M}_{\rm g\acute{a}s} \propto \mathcal{M}_{\rm d}$; : $\mathcal{M}_d \propto Y_{SZ}^{3/5}$
- Examples found in the literature:

$$\mathcal{M}_{500} = \frac{C \times 10^{14}}{E^{2/5}(z)} \left(\frac{Y_X [\text{keV } M_\odot]}{4 \times 10^{13}} \right)^{\alpha} h_{70}^{-1} M_\odot \quad \begin{cases} C = 1.175\,;\ \alpha = 0.526\,;\ (\text{Nagai et al., 2007}) \\ C = 1.12\ ;\ \alpha = 0.586\,;\ (\text{Sun et al., 2009})\,, \end{cases}$$

Very popular due to relatively small scatter

Scaling relations

- Cosmology is important for distant clusters.
- Scaling relations that depends on the density:
  - ✓ The density of clusters, inside the virial radius (about R200) is proportional to the mean density of the universe, that is, the critical density at z :
    $$\rho_c = \frac{3H^2(z)}{8\pi G}$$
  - ✓ Therefore, we have: $\rho_0 = \Delta \times \rho_c \propto E^2(z)$; $H(z) = H_0 E(z)$
    where $\Delta \sim 200$ (virial radius).
  - ✓ Since $M_g \propto \rho_0 R_c^3$; $L_X \propto \rho_0^2 R_c^3 T^{1/2}$; $M_d \propto R_c T$
    and assuming M_g/M_d constant ("faire sample" hypothesis) then:
    $$L_X \propto E(z) T^2 \;\text{ e }\; L_X \propto E^{7/3}(z) M_d^{4/3}$$
  - ✓ For a EdS universe, $E(z) = (1+z)^{3/2}$ (as we find in older papers).

Scaling relations

- By combining different scaling relations some degeneracy may be broken
- **Bulk flow** motion within about 400 Mpc may influence variables distance-dependent (that depends on Hubble-Lemaître law).
- Migkas+2021 applied a combination of scaling relations with 570 clusters to map a possible **spatial anisotropy**, expressed as an **apparent** (nearly) dipole of H_0.

Bulk flow motion $\approx$ 900km/s?

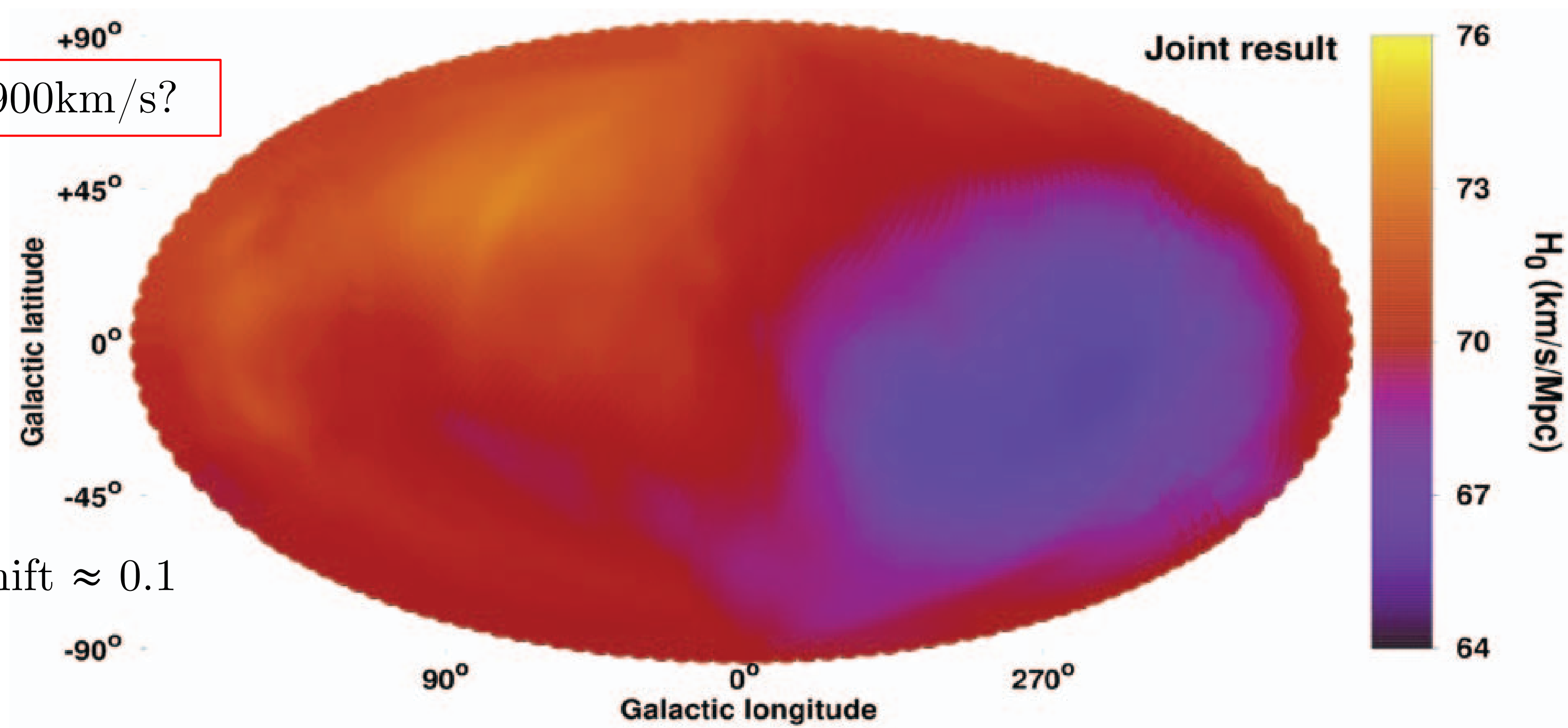

Median clusters redshift $\approx$ 0.1

Deep imaging: dynamical activity

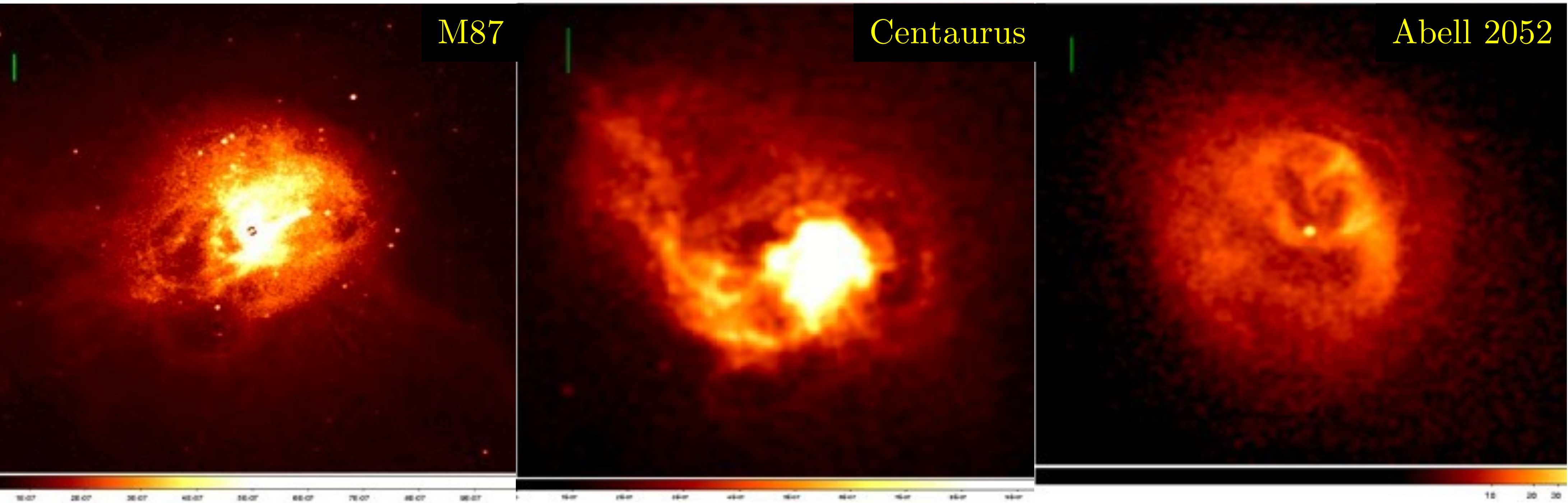

- Surface brightness of nearby cluster ($\propto$ projected n^2).
- Lots of structures, many due to non-gravitational processes (AGN feedback, sloshing and shocks)
- ➔ How cluster dynamical activity affects galaxy evolution?

Major collisions: Dissociative clusters in which the gas has been detached from the collisionless components

- 1E 0657-56 (Markevitch et al. 2004), “Bullet Cluster”
- MACS J0025.4-1222 (Bradac et al. 2008), “Baby Bullet”
- Abell 520 (Mahdavi et al. 2007), “Train Wreck”
- Abell 2744 (Merten et al. 2011), “Pandora Cluster”
- Abell S1063 (Gomez et al. 2012)
- Abell 2163 (Okabe et al. 2011)
- Abell 1758N (Ragozzine et al. 2011)
- DLSCL J 0916.2+2951 (Dawson 2012),“Musket Ball Cluster”
- ACT-CL J0102-4915 (Jee et al. 2014), “El Gordo”
- Abell 2319 (Storm et al. 2015)
- MACS J0744.0+9327 (Wilber et al. 2018)

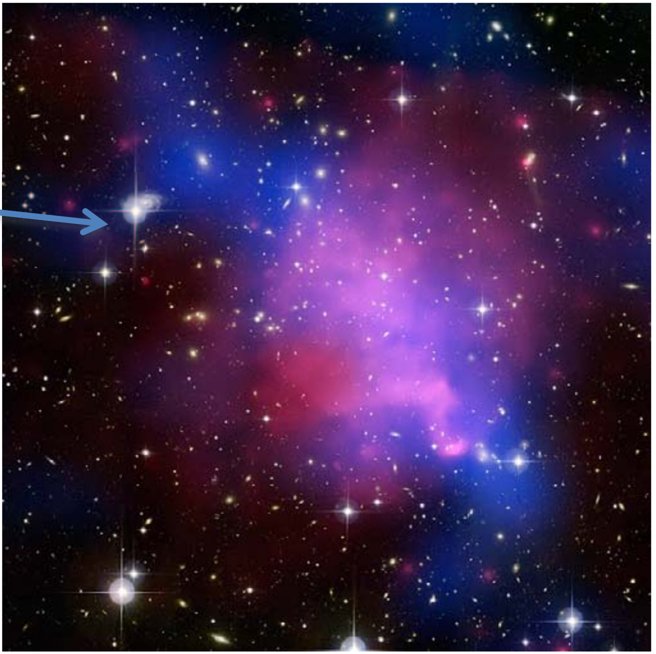

This is only a small subsample of colliding/merging clusters

simulated

“The Galaxy Cluster Merger Catalog”
ZuHone et al. 2018, ApJSuppl
http://gcmc.hub.yt.

Most famous example: the bullet cluster

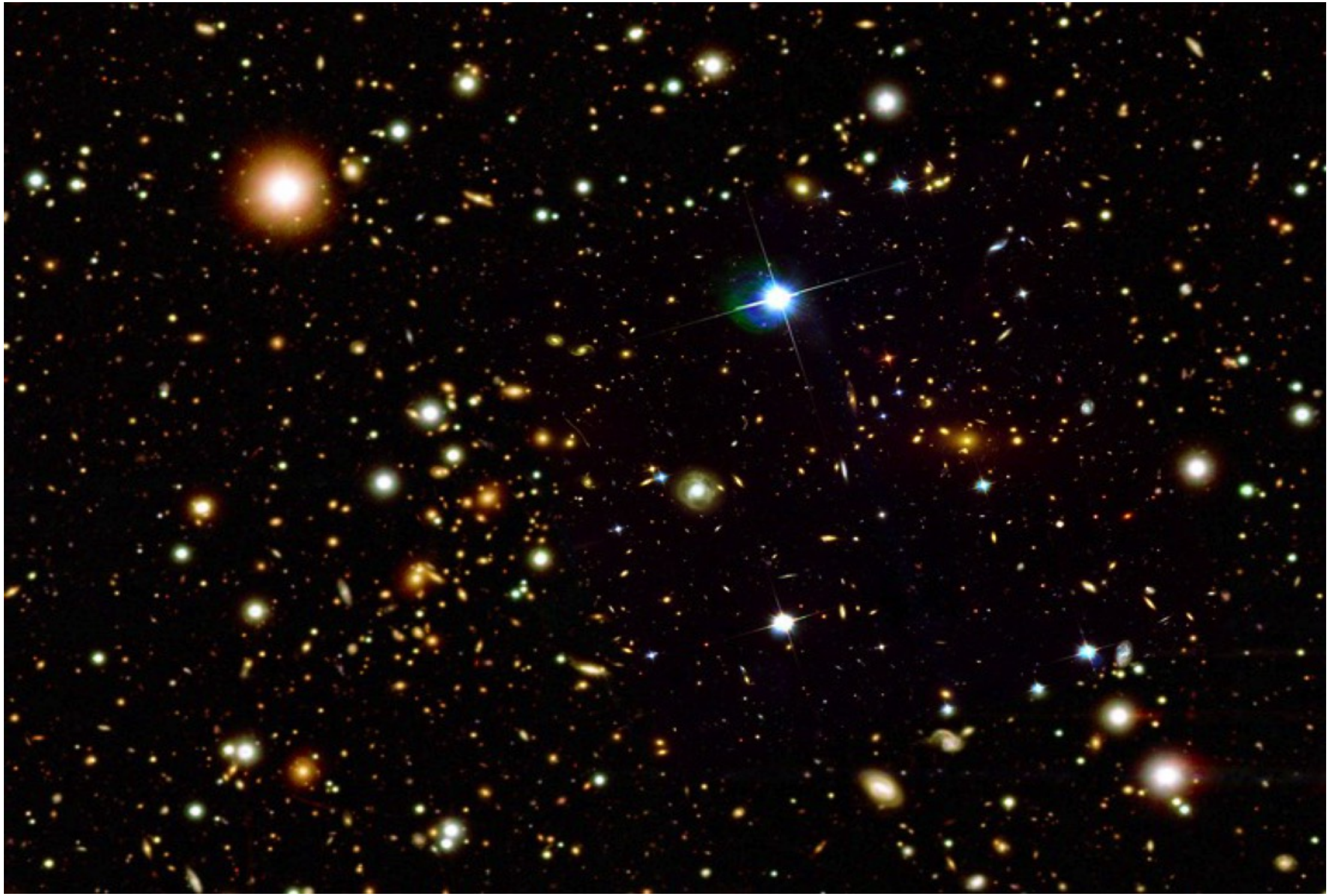

- Massive cluster at redshift $z = 0.3$.

Image NASA/STScI, Magellan/U.Arizona/D.Clowe et al. 2006

Most famous example: the bullet cluster

- X-ray emission map → diffuse gas ($kT \sim 14$ keV, $n \sim 10^{-2}$ cm^{-3}).
- Bow-shock → supersonic collision of 2 clusters.

X-ray NASA/CXC/CfA/M.Markevitch et al.

Most famous example: the bullet cluster

In clusters the gas mass is ~6x larger than the mass in galaxies.

One of the best evidences of dark matter.

- Mass distribution through weak-lensing effect.
- Mass distribution does not coincide with gas distribution (almost the same as the galaxy distribution).

Weak lensmass map: NASA/STScI, ESO WFI, Magellan/U.Arizona/Clowe et

Bow shock and cold front

- Bow shock
  => ρ ⬆, T ⬆.

- Cold front
  (contact discontinuity)
  => ρ ⬆, T ⬇.

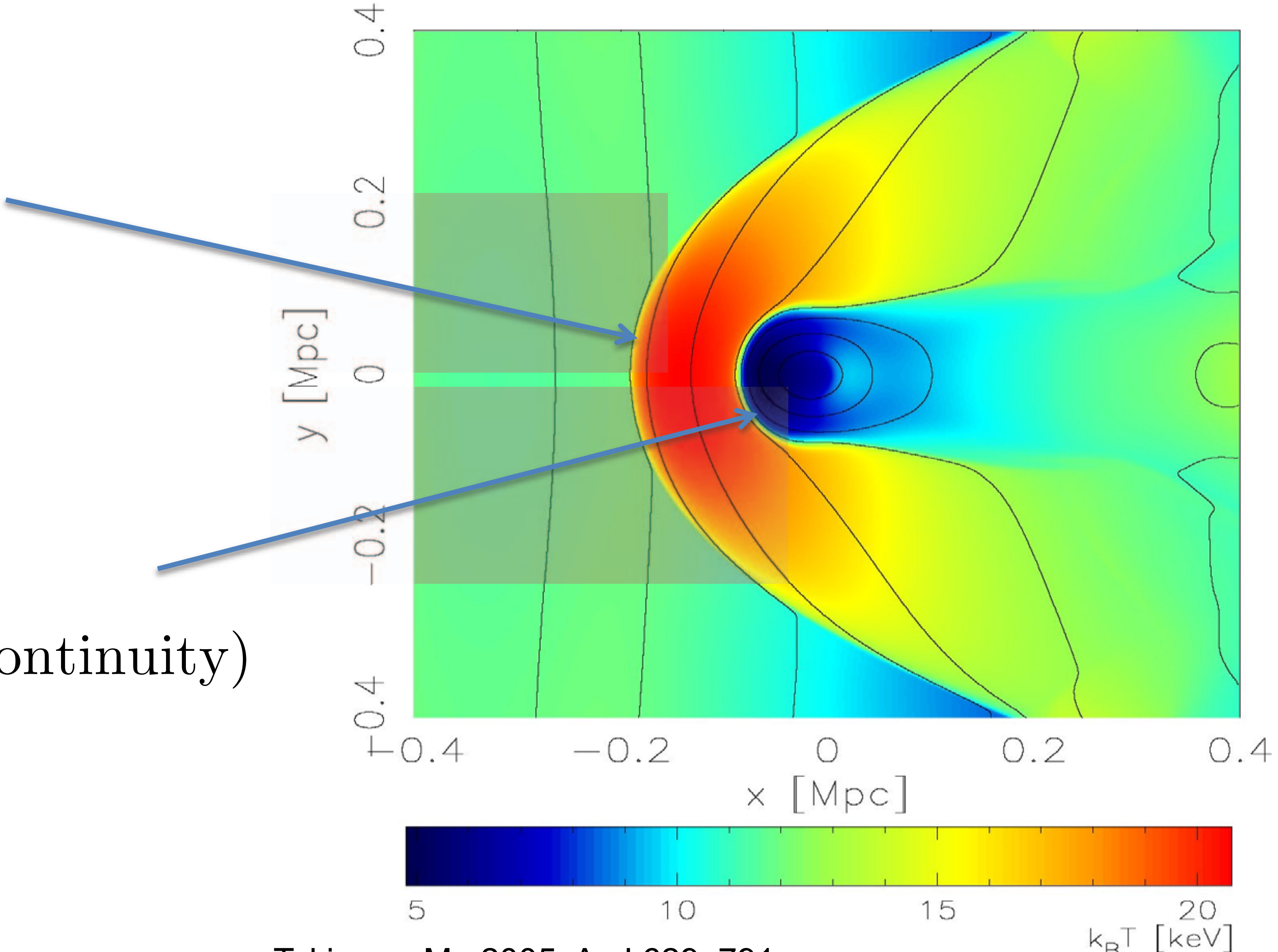

Takizawa M., 2005, ApJ 629, 791

Cross section of dark matter particles

- Markevich et al. (2004): ***scattering depth*** **(τ)**, similar to the optical depth, measures **how non-collisional the dark matter can be**.
  - ✓ $\tau \ll 1$ non-collisional; $\tau \gg 1$ collisional (such as the ICM gas).
- τ is estimated as:

$$\tau_s = \sigma \frac{N}{A} = \frac{\sigma}{m} \Sigma_s$$

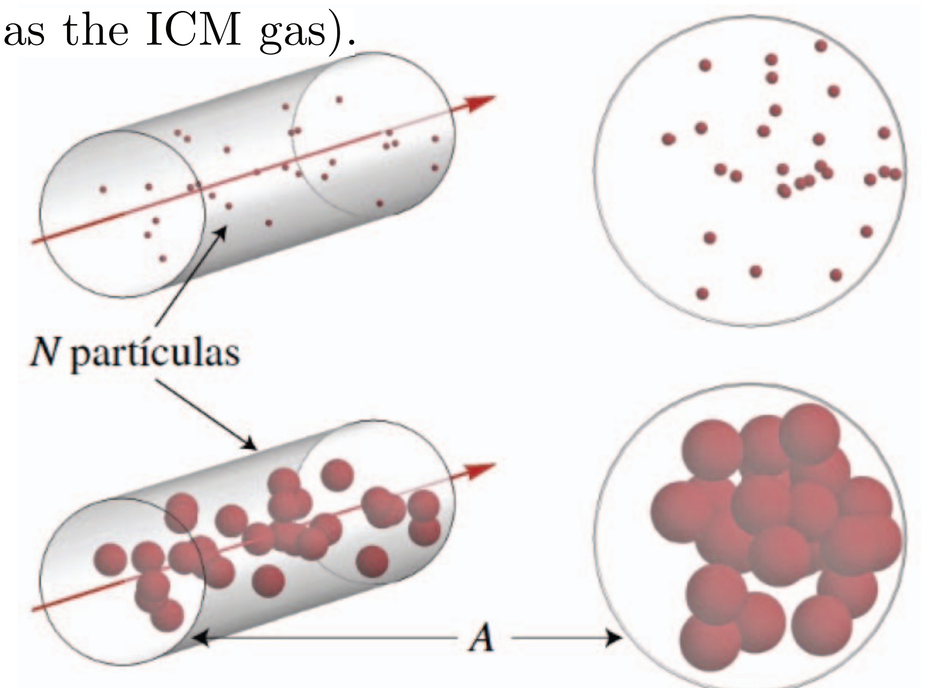

σ is the cross section, m the dark matter particle mass, and Σ_s the superficial density, $\Sigma_s = N\, m/A$, where A is the area that contains N particles.

- If dark matter is non-collisional (when we observe the **dissociation** between the ICM gas and matter distribution), $\tau < 1$, and we have a superior limit to the ratio σ/m.
- Typically, in **dissociative clusters**, $\sigma/m < 1$–$5\ \mathrm{cm}^2\, \mathrm{g}^{-1}$ (e.g. Eckert+2022)

Search of high-z ($z > 1$) clusters

- Probe cosmological parameters, dark energy equation of state (w).
- Evolution of galaxies in high density environment.
- Structure formation: observe forming clusters.
- Need of a large sample. Need to **find** them!

Some difficulties:

- At $z = 1$:
  - ✓ Core (≈100 kpc) ≈ 15'' (only Chandra can resolve it);
  - ✓ 1 photon [0.5-8.0 keV] band each 20 secs.
    (assuming $L_X \approx 2\text{x}10^{45}$ erg/s and $kT = 6$ keV);
  - ✓ Huge "foreground" contamination in galaxy distribution;
  - ✓ L_* galaxy has magnitude $r \approx 22$.

Above all, very few rich clusters are expected at $z > 1$
(at least with the current LCDM scenario)

Press-Schechter mass function

- The Press-Schechter (1974) formalism (and later, more precise versions) can be used to compute the number of collapsed halos for different redshifts.

- Test different cosmological scenarios. How many rich cluster formed at $z = 1$?

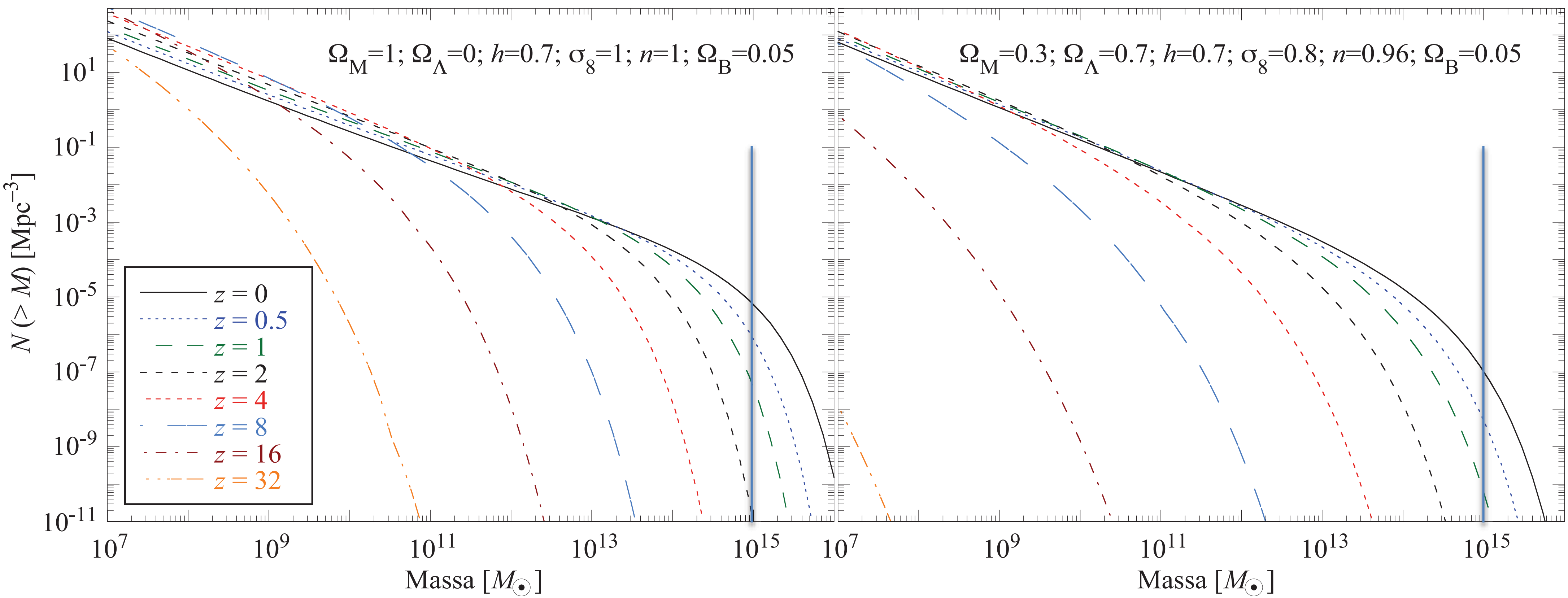

Some SDSS clusters
at different z.

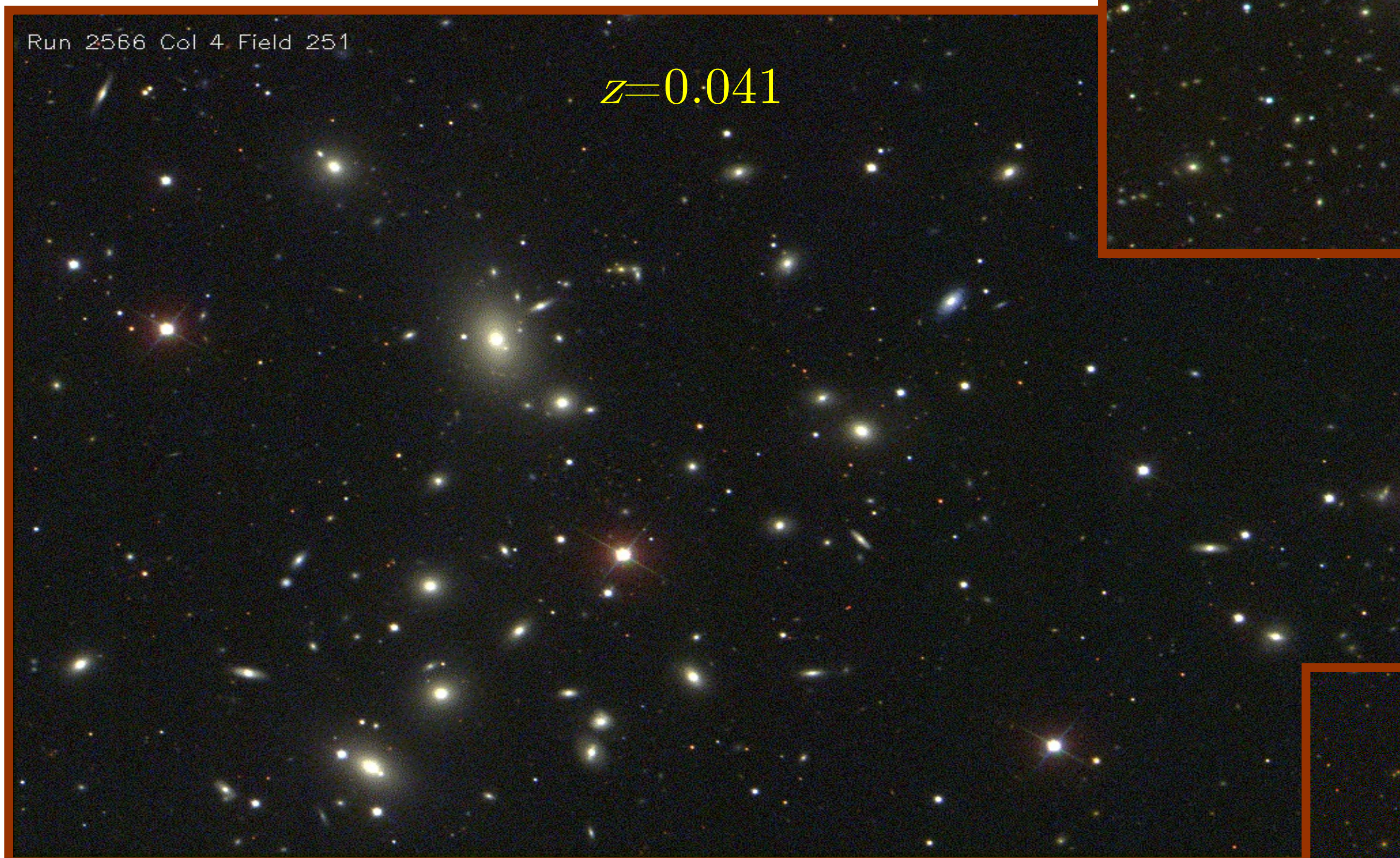

Optical observation, 2.5m telescope

How to find high-z cluster

- X-ray emission
  - ✓ non-resolved sources ROSAT, XMM (@ $z \approx 1$)
  - ✓ Low count rate (10s to 100s of ks exposures)
  - ✓ Search in archive pointed observations (ROSAT, *Chandra*, XMM)
  - ✓ XMM-LSS survey

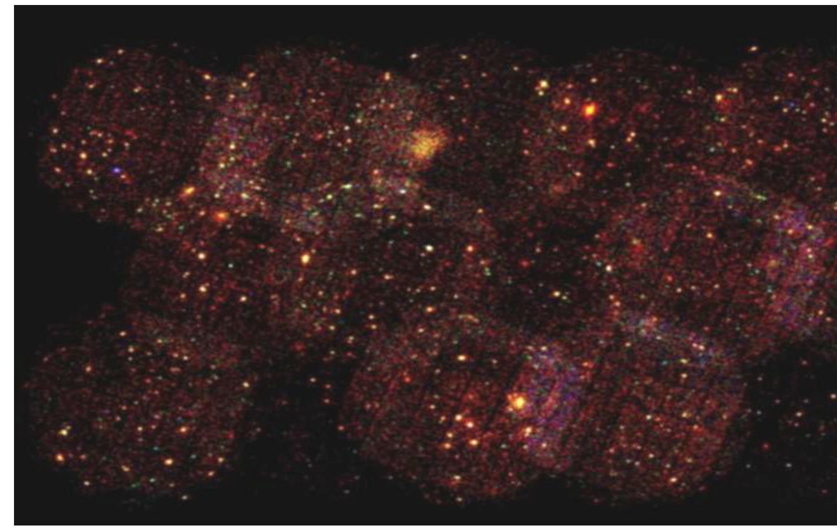

- Sunyaev-Zel'dovich Effect
  - ✓ Clusters appear as cold spots over the CMB at $\nu < 200$ GHz;
  - ✓ Signal independent of distance (no cosmological dimming, Reese 2003; Planck collab. 2018).
- Search clusters near radio-galaxies/QSOs
  - ✓ Lots of AGNs at the outer region of clusters
  - ✓ Central galaxy in a rich clusters is often a radio source (Crawford & Fabian 1996; Dickinson 1997; Best 2000).
- Color-magnitude relation
  - ✓ Elliptical galaxies in clusters from a tight "red-sequence" in the colour-magnitude plane;
  - ✓ Example: Red-Sequence Cluster Survey (Gladders & Yee 2000, 2005).

How to find high-z (proto-cluster)

- ODIN: Identifying Protoclusters and Cosmic Filaments Traced by **Lyα-emitting (LAE) Galaxies** (Ramakrishnan+2024)
  - ✓ DECam
  - ✓ typical z = 3

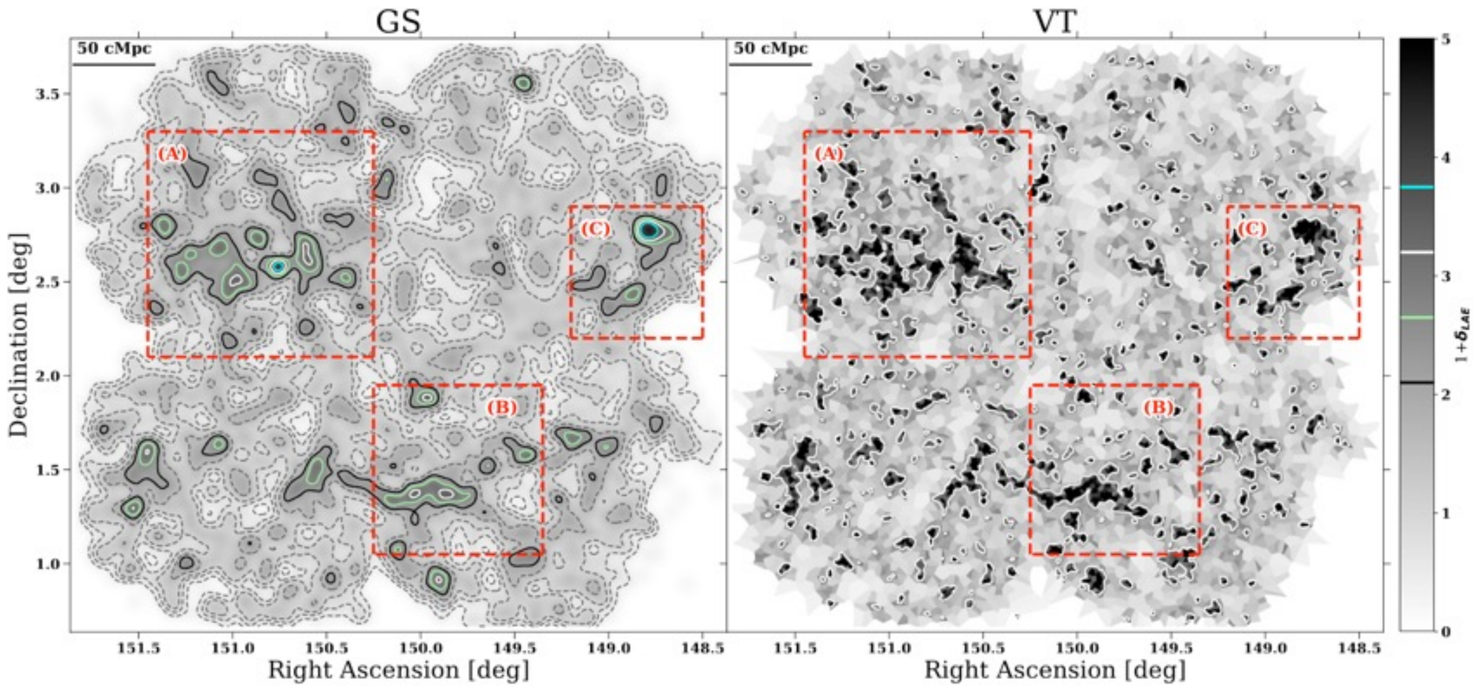

How to find high-z (proto-cluster)

- Submillimeter galaxies (SMG) as tracers.
- Dust enshrouded star-forming galaxies.

- Calvi et al. (2023) detect overdensities around 11/12 SMG in 8 large scale proto-clusters.
  Complex morphology inside 0.4—1.0 Mpc.
- da Costa, Delmestre & Gonçalves (2022): SMGs trace typical moderate-mass structures instead of the more massive, Coma-like clusters progenitors.
- Araya-Araya et al. (2024): apply the L-GALAXIES semi-analytic model (SAM) to the Millennium N-body Simulation. Confirm SMG as tracers of proto-clusters. Overdense environments have a relative overdensity of high-mass halos and `oversample' the high-mass end of the star formation.

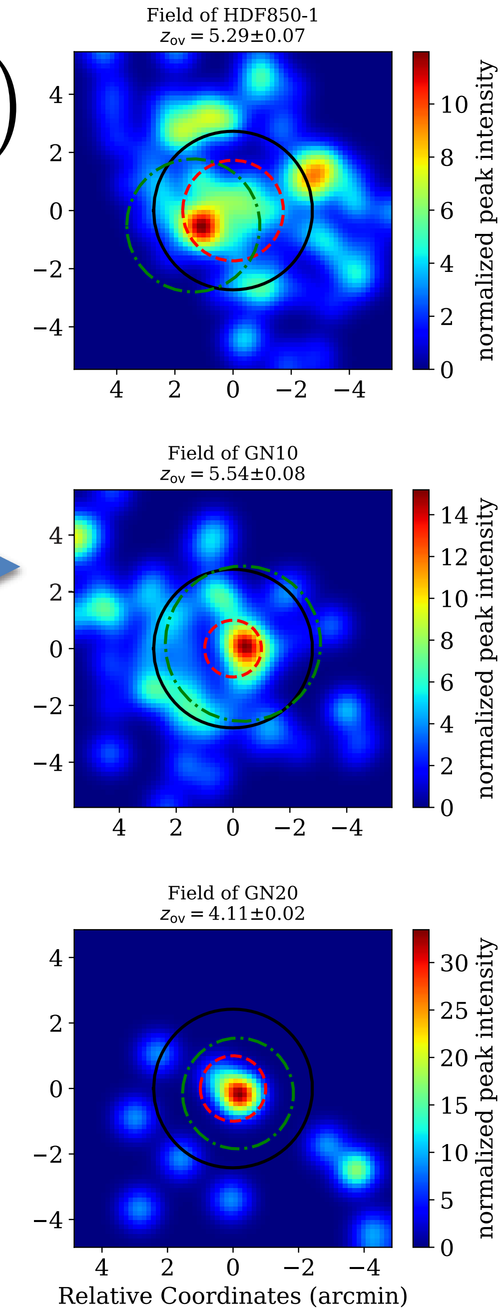

Some of the most distant clusters known

spectroscopically confirmed + X-ray signature

#	z	Name	Sel.	$L_{X,500,bol}$ 10^{44} erg/s	M_{200} $10^{14} M_{sun}$	References
1	2.07	CL J1449+0856	MIR	0.9	0.7	Gobat+11
2	1.75	XMMU J1053+5723	Xray	0.5	0.6	Henry+10
3	1.75	IDCS J1426-3508	MIR	16	4.1	Stanford+12, Brodwin+12
4	1.62	XCL J0218-0510	Xray	0.4	0.7	Tanaka+10, Pierre+11, Papovich+10
5	1.58	**XDCP J0044.0-2033**	**Xray**	**6.1**	**3.0**	Santos+11
6	1.56	**XDCP J1007.3+1237**	**Xray**	**2.1**	**1.7**	Fassbender+11
7	1.49	**XDCP J0338.8+0021**	**Xray**	**1.1**	**1.2**	Nastasi+11
8	1.49	ISCS J1432.4+3250	SZ	3.5	2.5	Brodwin+10
9	1.46	**XCS J2215.9-1738**	**Xray**	**2.2**	**2.0**	Hilton+10, Stanford+06, Bielby+10
10	1.41	ISCS J1438.1+3414	SZ	2.2	2.2	Brodwin+10, Stanford+05

Rene Fassbender & Piero Rosati 2012
Strazzullo et al. 2019

Some high-z clusters

- RX J0848.9+4452 (one of the earliest discovered)
- Rosati et al. 1999, $z = 1.27$

- Evolution of the colour-magnitude relation (Holden et al. 2004)
- Large scale environment (Heines et al. 2004)
- Evolution of scaling relations (Ettori et al. 2004)

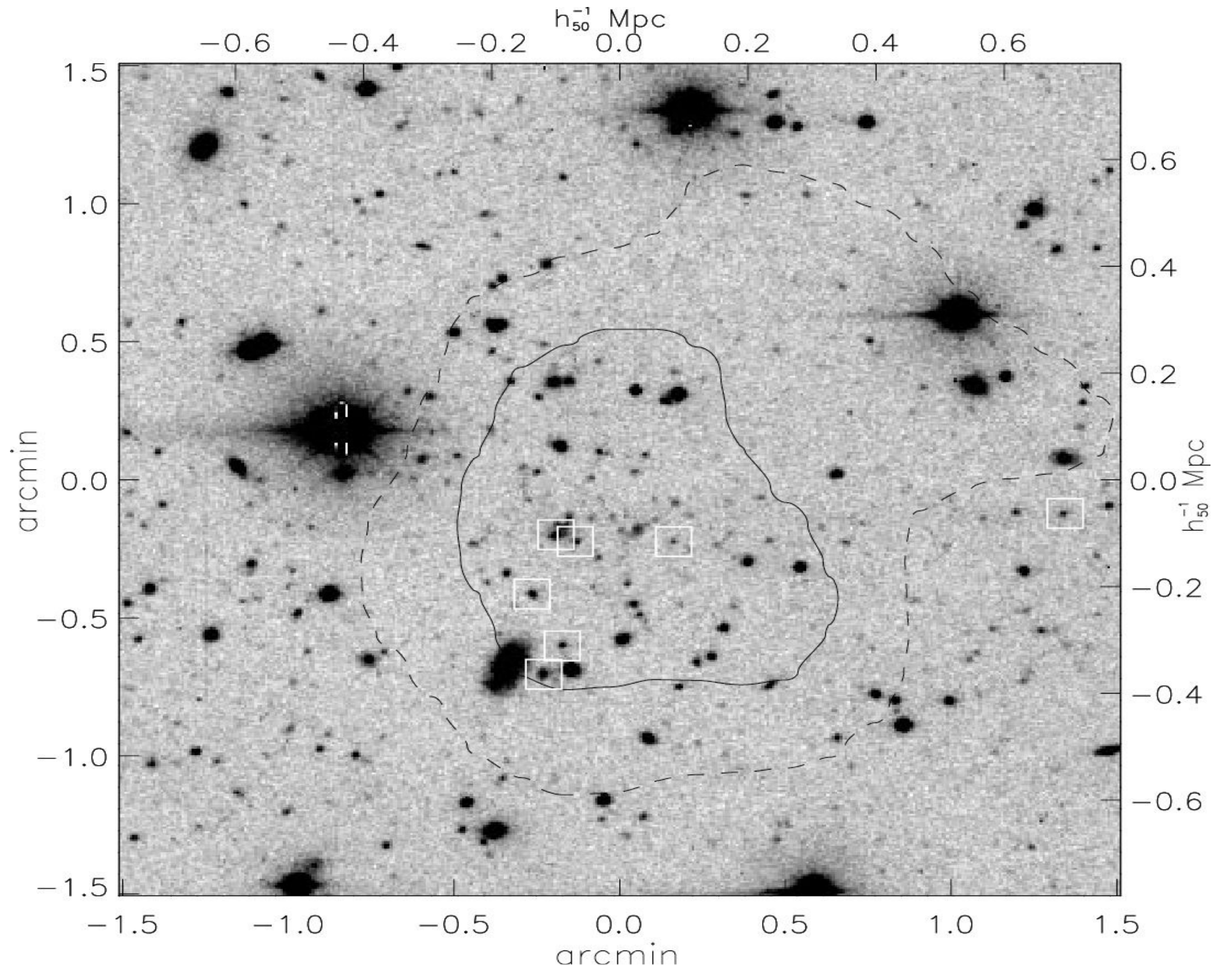

Some high-z clusters

- RX J1053.4+5735, z = 1.26
- Hashimoto et al. 2002 – Found with X-ray in the Lockman Hole
- XMM deep imaging shows bimodal structure.

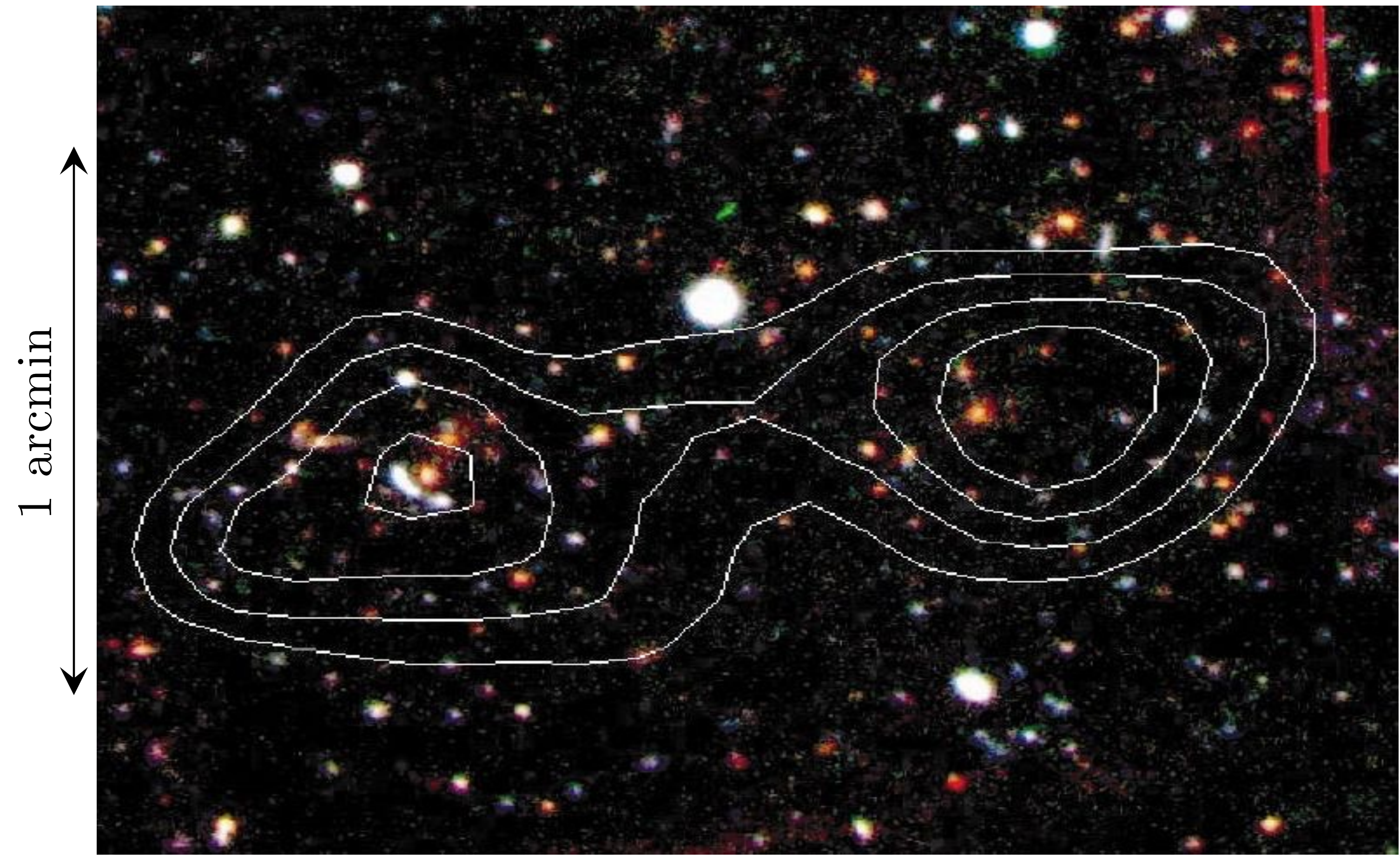

Most distant know cluster

- Cl J1001 (W16) at z = 2.506 (spec) [Wang+2016]
- X-ray detected
- Strong concentration of radiogalaxies (Daddi+2018)

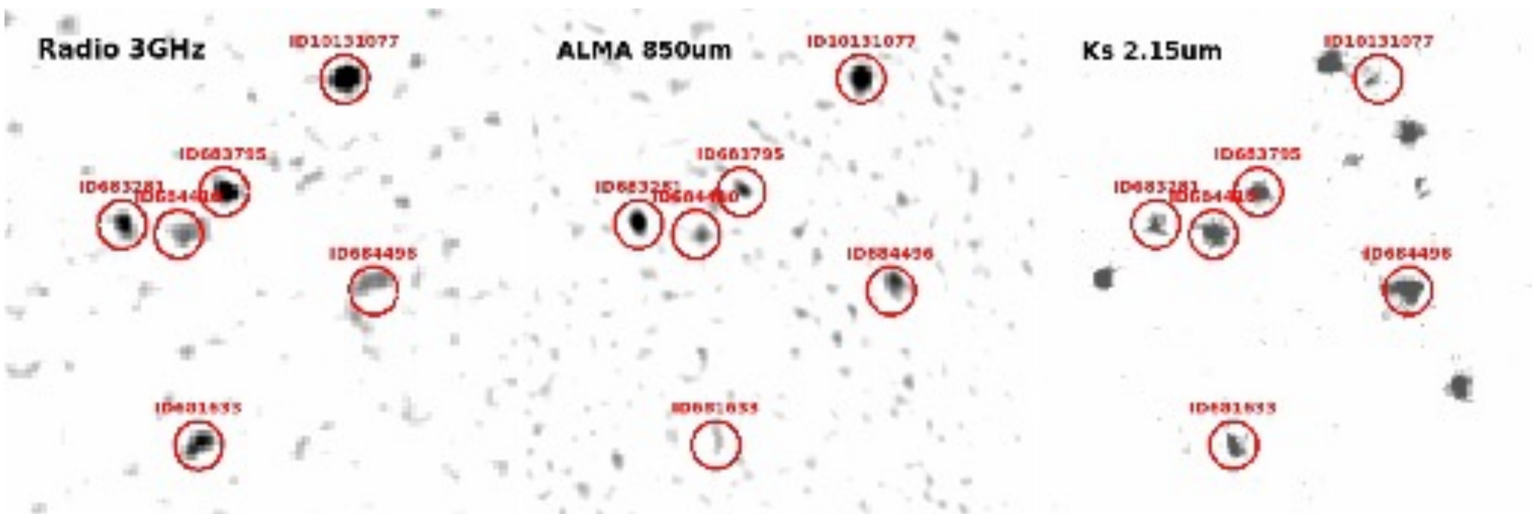

Proto-clusters turning into cluster

PKS 1138–262 ($z = 2.156$; commonly known as the Spiderweb galaxy

HST + VLA (red) + VLT(pink) + SZ(Alma+VLA, blue)

ICM detected by SZ, not X-ray.

The SZ effect offset with respect to the Spiderweb galaxy suggests that the protocluster core is undergoing a dynamically active phase.

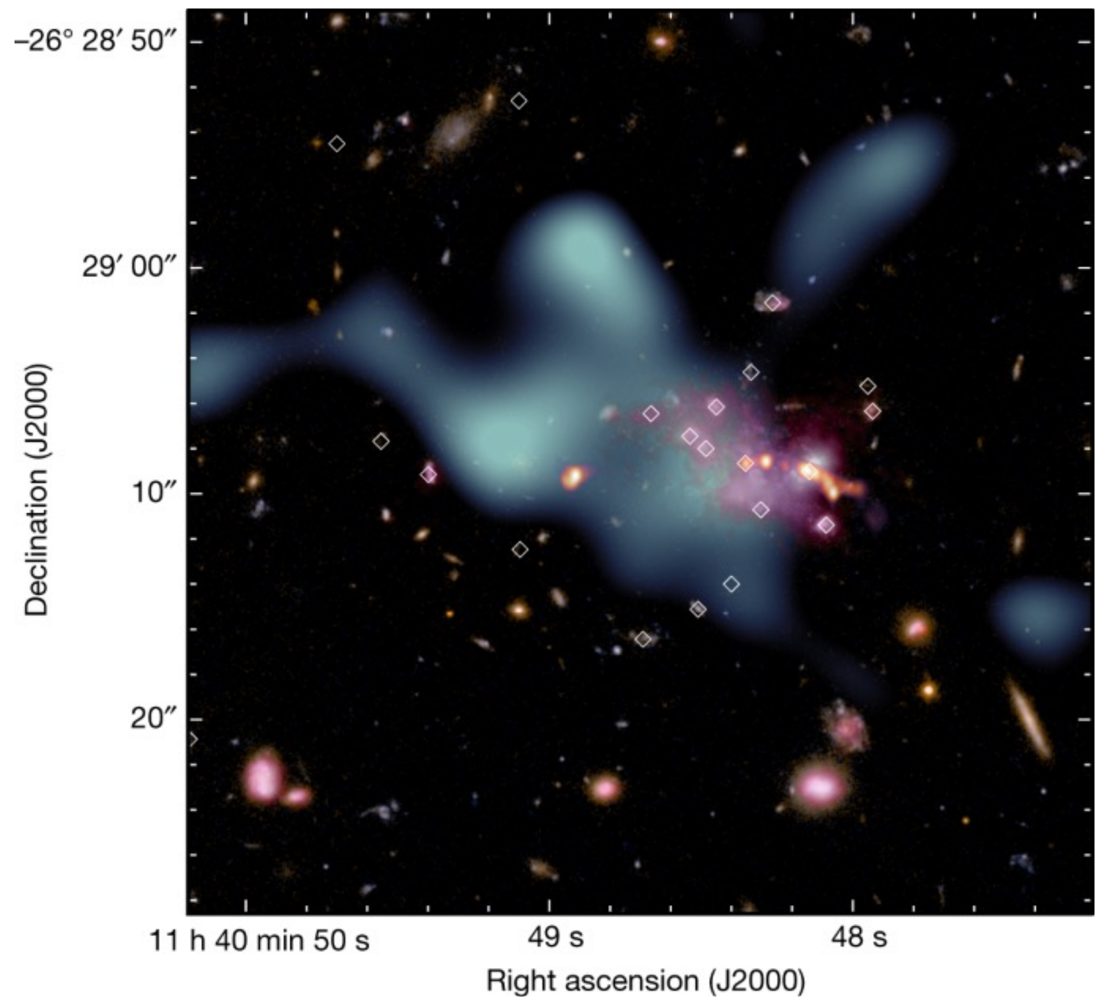

Di Mascolo+2023

X-ray astronomy

- Chandra: launched in 07/1999
  - ✓ March 2024: announce of plans for major reductions for Chandra budget → probably will end in 2026
- XMM-Newton: launched in 12/1999
  - ✓ scheduled to operate until the end of 2026
  - ✓ EPIC camera has lost 2 CCDs
- Suzaku: launched in 07/2005
  - ✓ large spectral range (up to 600 keV), large field of view
  - ✓ Ended in 09/2015

- Very extensive data archive, hundreds of clusters and groups observed
  - ✓ Data mining is an important tool

eROSITA

(J-PAS collaboration)

- Launched 07/2019 from Baikonur, part of Spektr-RG (Russian mission).
  - ✓ First prevision launch aimed for 2012.
  - ✓ Successor of ABRIXAS, lost during launch in 1999.
- Placed at L2 for an all-sky survey, 25x deeper than RASS (ROSAT All-Sky Survey). 4 years for the survey + 3 of pointed observations.
- DR1: 01/2024 (only German half).

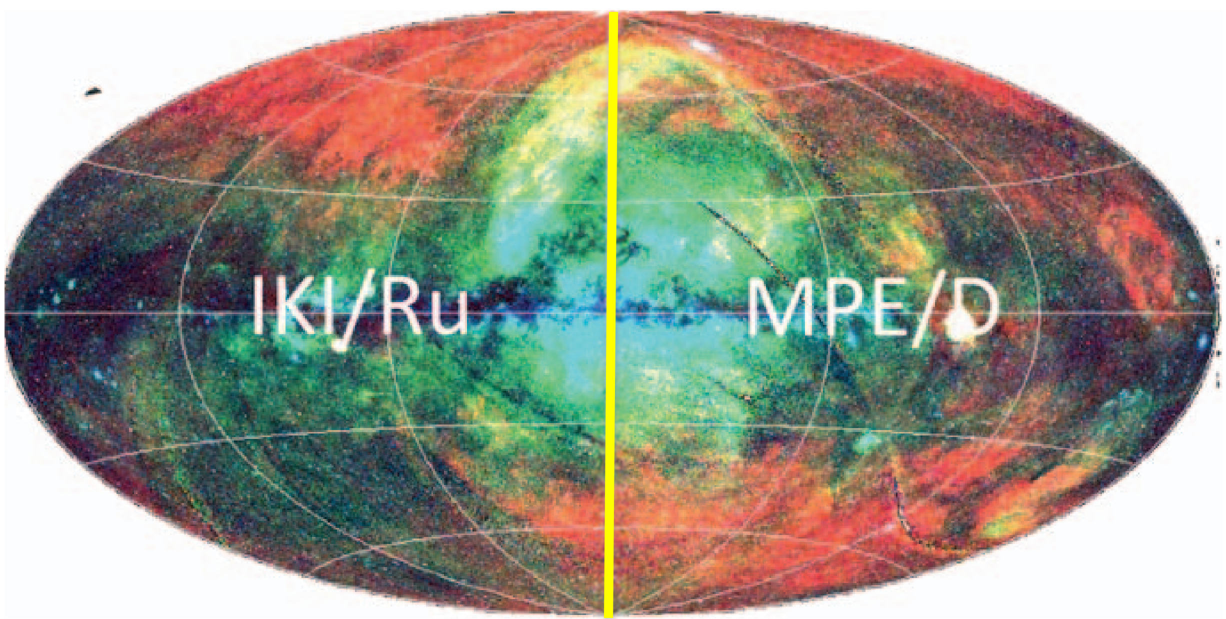

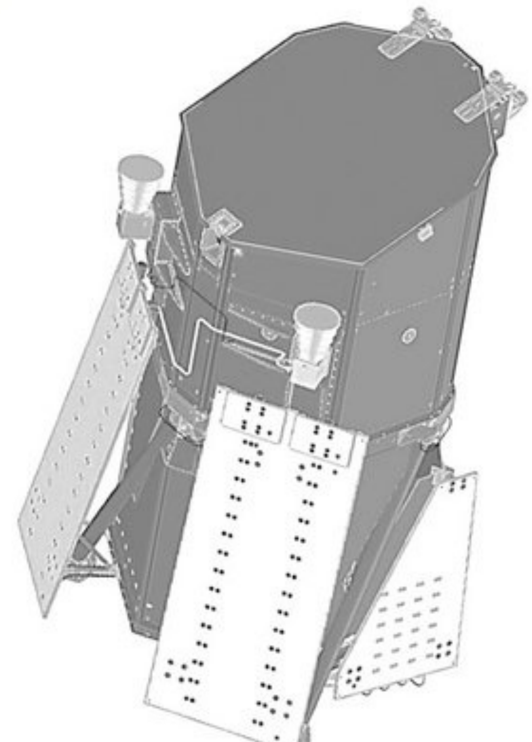

http://www.mpe.mpg.de/eROSITA https://erosita.mpe.mpg.de/dr1/erodat/skyview/sky/

ATHENA

Advanced **T**elescope for **H**igh **EN**ergy **A**strophysics

- Selected in 2014 by ESA to become an L2 mission of its *Cosmic Vision programme*, planned launch in 2037 (initially planned for 2028), minimum duration 4 years.
- Effective area 1.4 m^2 (initially planned 3.4 m^2).
  - ✓ XMM-Newton has a bit less than 0.5 m^2.
- X-ray Integral Field Unit (X-IFU), energy resolution 2.5 eV, spatial 5″, fov 5′.
- Wide Field Imager (WFI), 40x40′, spatial resolution de 5″.

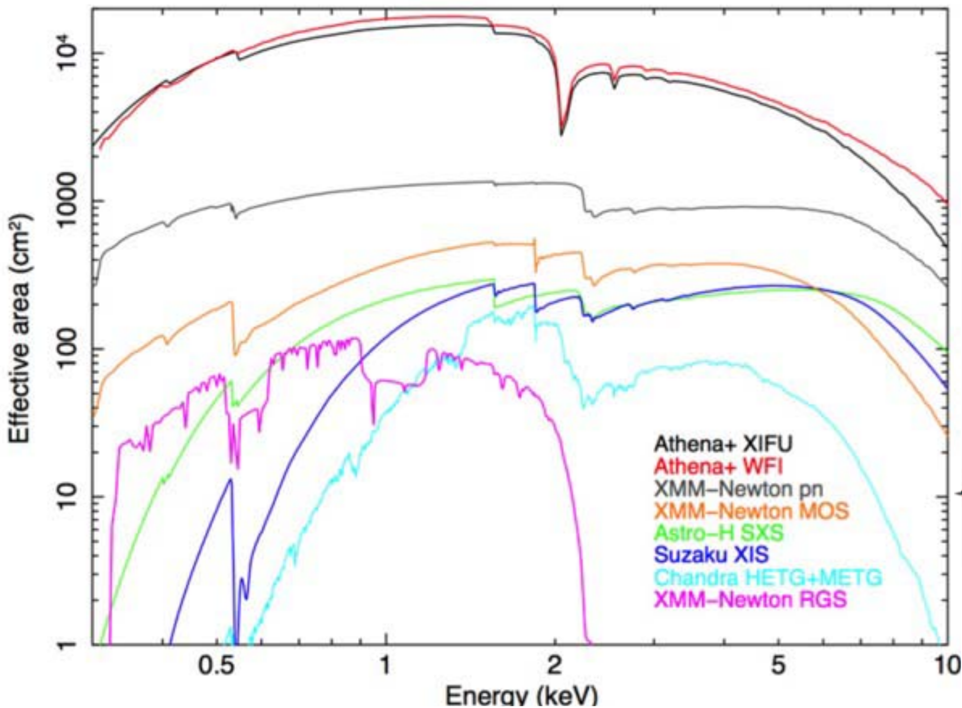

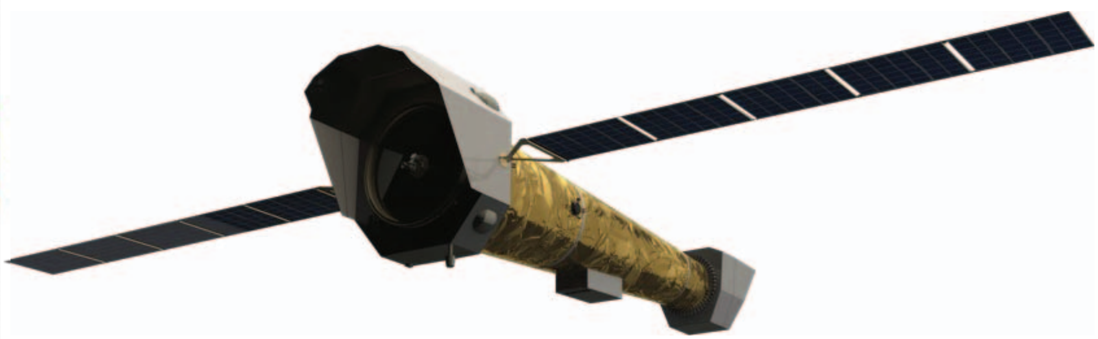

http://www.the-athena-x-ray-observatory.eu/